A New Perylene Monoimide Derivative as Potential DNA–Binding Agent

Ziyad Ahmed Shareef

Submitted to the
Institute of Graduate Studies and Research
in partial fulfillment of the requirements for the Degree of

Master of Science
in
Chemistry

Eastern Mediterranean University
July 2014
Gazimağusa, North Cyprus

Approval of the Institute of Graduate Studies and Research

Prof. Dr. Elvan Yılmaz
Director

I certify that this thesis satisfies the requirements as a thesis for the degree of Master of Science in Chemistry.

Prof. Dr. Mustafa Halilsoy
Chair, Department of Chemistry

We certify that we have read this thesis and that in our opinion it is fully adequate in scope and quality as a thesis for the degree of Master of Science in Chemistry.

Prof. Dr. Huriye İcil
Supervisor

Examining Committee

1. Prof. Dr. Huriye İcil

2. Asst. Prof. Dr. Nur P. Aydınlık

3. Asst. Prof. Dr. Mustafa E. Özser

ABSTRACT

Nowadays, inhibiting telomerase and consequent disruption of the telomeres *via* formation of small organic molecule based G-quadruplex DNA structures is extensively studied. The potential of curing cancer cells (preventing the replication) by the formation of G-quadruplexes is emerging as an efficient method.

π-Conjugated perylene dyes are one of the most suitable small organic molecules that can bind to DNA to form G-quadruplexes. In the present research work, two perylene dyes, namely, aminododecyl perylene diimide (ADPDI) and aminododecyl perylene monoimide (ADPMI) were synthesized in order to explore their potential towards DNA binding. Especially, long alkyl chain attached amino groups have been induced at the imide positions of the perylene chromophore to increase the capacity of hydrogen bonding.

The synthesized ADPDI and ADPMI dyes have been characterized via TLC, FTIR, UV-vis, and emission measurements. FTIR spectra support the structure of the dyes. UV-vis absorption spectra in dipolar aprotic DMF (for ADPMI) and nonpolar isoquinoline (for ADPDI and ADPMI) solvents show that the dyes are aggregated to some extent in solutions by forming a broad absorption shoulder in their absorption spectra.

Keywords: Perylene diimide, Perylene monoimide, G-quadruplex, DNA binding

ÖZ

Günümüzde, G-quadruplex DNA yapıları kaynaklı küçük organik molekül oluşumu ile inhibe telomeraz ve telomerlerin bozulma sonuçları yaygın olarak incelenmektedir. G-quadruplex oluşumu ile kanser hücrelerinin tedavi potansiyeli (replikasyonu önlemede) etkin bir yöntem olarak ortaya çıkmaktadır.

π-konjuge perilen boyaları, G-quadruplexes oluşturması için DNA'ya bağlanmaya en uygun küçük organik moleküllerden biridirler. Bu çalışmada, iki perilen boyası; Aminododesil perilen diimit (ADPDI) ve Aminododesil perilen monoimit (ADPMI) DNA'ya doğru bağlanma potansiyellerini keşfetmek amacıyla sentezlenmiştir. Özellikle, uzun alkil zinciri bağlı amino grupları, Hidrojen bağlama kapasitesini artırmak için perilen kromoforunun imit pozisyonlarına bağlanmıştır.

Sentezlenen ADPDI ve ADPMI boyaları, TLC, FT-IR, UV-Visible ve Emisyon ölçümleri ile karakterize edilmişlerdir. FT-IR spektrumu sentezlenen boyaların yapısını ispat etmektedir. UV-Visible absorpsiyon spektrumu, dipolar aprotik DMF (ADPMI) ve polar olmayan izokinonin (ADPDI ve ADPMI) çözgenlerindeki boyaların absorpsiyon spektrumlarında çözeltilerdeki bazı yaymalar ile birleşme (agregasyon) olduğunu, bunu geniş bir omuz oluşturarak göstermektedir.

Anahtar Kelimeler: Perilen diimid, Perilen monoimid, G-quadruplex, DNA bağlama

TO MY FAMILY

ACKNOWLEDGMENT

The first and foremost thing is to declare my deep gratefulness to my supervisor Prof. Dr. Huriye İcil for allotting this interesting subject and for her productive guidance toward completing the project. Besides, it is a great opportunity to learn organic chemistry from her. I am also indebted for her moral in general life.

I am also very thankful to the family of Organic Group at Eastern Mediterranean University.

I am indebted to my family for their complete encouragement.

TABLE OF CONTENTS

LIST OF TABLES

LIST OF FIGURES

LIST OF SCHEMES

LIST OF SYMBOLS/ABBREVIATIONS

$\overset{o}{A}$	Armstrong
A	Adenine
A	Absorption
ADPDI	N,N′-Bis(12-aminododecyl)-3,4,9,10-perylenebis-(dicarboximide)
ADPMI	N-(12-aminododecyl)-3,4,9,10-perylene-tetracarboxylic-3,4-anhydride-9,10-imide
AU	Arbitrary unit
C	Cytosine
c	Concentration
DMF	N,N′-dimethylformamide
DMSO	Dimethyl sulfoxide
DSC	Differential scanning calorimetry
ε	Molar Absorption coefficient
ε_{max}	Maximum Extinction coefficient/Molar absorptivity
eV	Electron volt
E_g	Band gap energy
f	Oscillator strength
FT-IR	Fourier transform infrared spectroscopy
G	Guanine
h	Hour
hν	Irradiation
HOMO	Highest occupied molecular orbital

IR	Infrared spectrum/spectroscopy
kcal	Kilocalorie
LUMO	Lowest unoccupied molecular orbital
M	Molar concentration
max	Maximum
min	Minimum
mol	Mole
mp	Melting point
n	Number of electrons (in the reduction process)
NMR	Nuclear Magnetic Resonance Spectroscopy
NMP	*N*-methylpyrrolidinone
τ_0	Natural radiative lifetime
THF	Tetrahydrofuran
T	Thymine
UV	Ultraviolet
UV-vis	Ultraviolet and visible light absorption
$\bar{\nu}$	Wavenumber
$\Delta\bar{\nu}_{1/2}$	Half-width (of the selected absorption)
$\bar{\nu}_{max}$	Maximum wavenumber/Mean frequency
V	Volt
λ	Wavelength
λ_{exc}	Excitation wavelength
λ_{em}	Emission wavelength
λ_{max}	Maximum wavelength

Chapter 1

INTRODUCTION

1.1 Introduction to Perylene and Perylene Derivatives

Perylene dyes are belonging to the rylene framework with conjugate double bonds (due to the successive aromatic units) and are shown in Figure 1.1. As shown in Figure 1.1, a simple perylene unit itself possesses two naphthalene units in an ordered pattern attached at its 'peri'-positions [1].

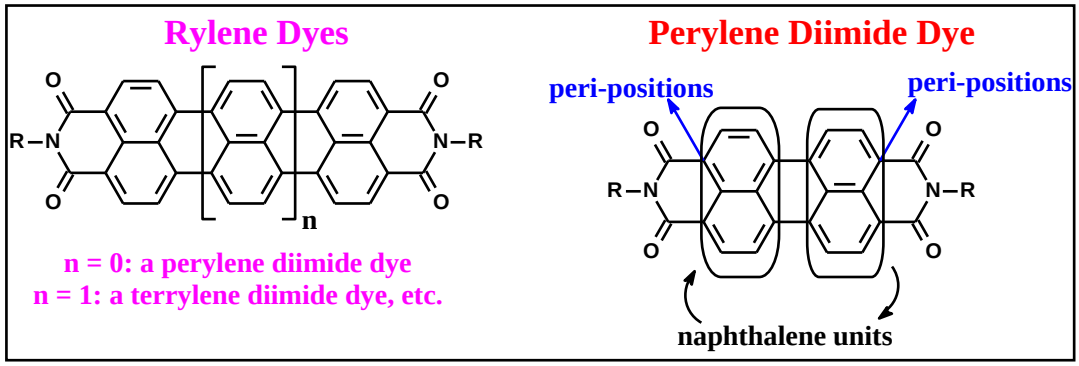

Figure 1.1: A General Structure of Higher Order Rylene Dye and Perylene Dye

Perylene dyes are proved to be very useful compounds in versatile fields such as engineering, medicine, electronics, and academia. The potential applications in many areas are based on: (a) their strong absorption of electromagnetic radiation at visible region, (b) exciting light emitting features with very high photoluminescence quantum yields (ϕ_f=1), (c) high chemical, electrochemical, thermal, mechanical stabilities, (d) excellent electron accepting nature with *n*-type character, (e) and tunable band gap energies [2-4].

The most credibility of perylene derivatives is subjected to its structure (explained in Figure 1.2) where the tailoring is possible at multiple positions.

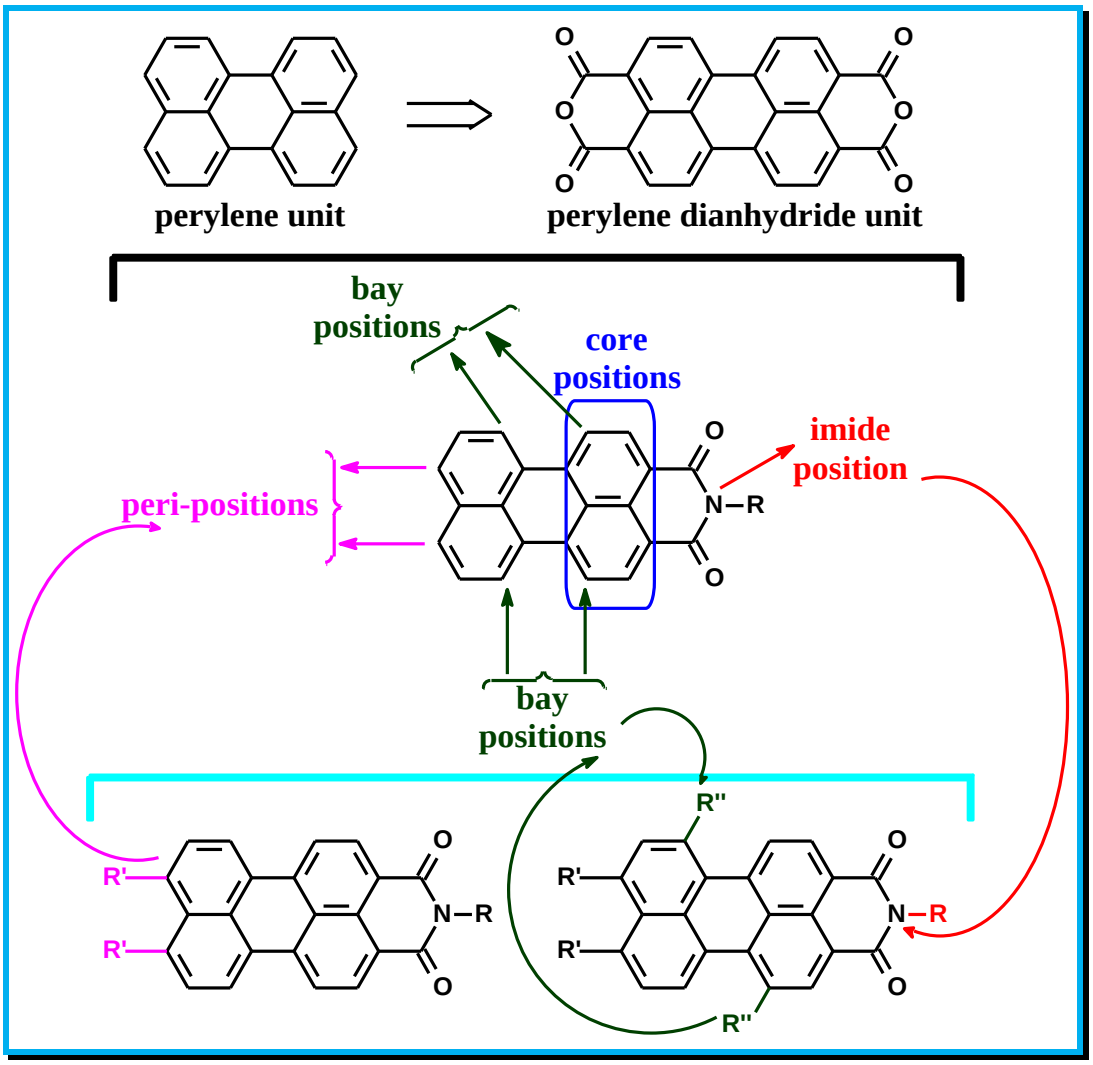

Figure 1.2: The Basic Raw Materials: A Perylene Unit (shown at top left) and a Perylene Dianhydride Unit (shown at top right); A General Pery-, Bay-, Core-, Imide-Substituted Perylene Dye Derivative (shown at center); and General Structures of Various Perylene Derivatives (shown at bottom)

When considered the applicability of perylene dyes, one of the most important uses of perylene dyes is their general light emitting character above 500 nm that contributes from the betterment of the signal-noise ratio in biologic systems due to the existence of the high auto-fluorescence of living organisms [5]. The cell-permeable ability of perylene dyes has been utilized to stain the living cells with

increased performance. Perylene dyes can be used potentially in fluorescent labelling applications with their high-fluorescence quantum yields and photostabilities. Such dyes can be attached to DNA as they are potential ligands which induce stability to G-quadruplex structures. In addition, hydrosoluble perylene chromophoric dyes assist π–π stacking interactions with the terminal G-tetrad groups of G-quadruplex DNA [6-9].

1.2 G-Quadruplex DNA

G-quadruplexes are the folded DNA sequences and are four stranded (shown in Figure 1.3) secondary structures made up of guanine (G) bases (Figure 1.3). Hence they are also referred as DNA quadruplexes [10-11].

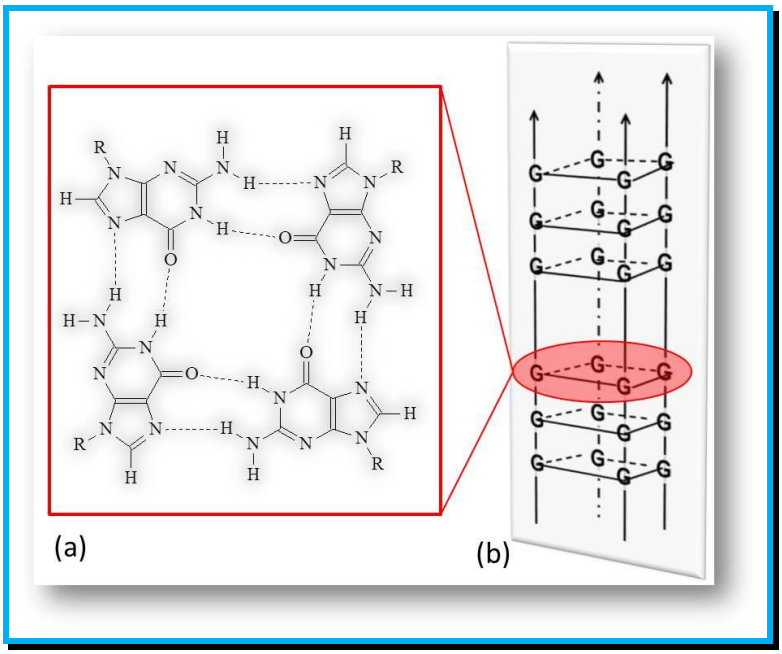

Figure 1.3: Representation of a (A) G-tetrad Containing Planar Four Guanine (G) Bases Arranged through Eight Hydrogen Bonds and (B) Structure of G-quadruplex where the Tetramolecular Parallel Stacks Stand for Single G-rich Repeating Units of DNA Strands

As shown in Figure 1.3A, the Guanine bases are capable of forming two hydrogen bonds along each edge (usually referred as Hoogsteen guanine base-pair hydrogen bonding) to form guanine tetrads. These tetrads can stack on each other and the

stacked tetrads held together by nonbonding π–π interactions to form G-quadruplex structure (Figure 1.3B) [6, 12-14].

In 1991, it was reported that small organic molecule based G-quadruplex DNA structures inhibit telomerase and consequently disrupt the telomeres. This has brought a big revolution in investigating the small organic molecules which could interact with G-quadruplexes. As a result, a variety of organic lead compounds (Figure 1.4) and their interactions with G-quadruplexes have been explored [15].

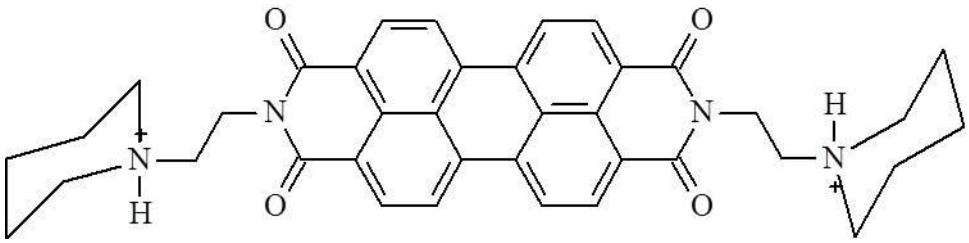

Figure 1.4: A Perylene Derivative (PIPER) Reported previously as an Efficient Structural Model for Formation of Intermolecular G-quadruplexes [15]

A key point involving the structural design and synthesis of ligands (that interact with DNA quadruplex) is to study the factors that enhance binding selectivity of G-quadruplexes. There are so many methodologies developed experimentally which can estimate the capability of ligands to form G-quadruplex structures such as NMR and X-ray structural identification. Although small organic molecule based G-quadruplex sequences were reported as potential anti-carcinogenic agents, they are limited in usage due to uncertain cytotoxic effects. In major cases, a kind of prognostic algorithm should be developed for identifying G-quadruplex targets on a scale of genomic level [11].

Recently, electrochemical analysis of DNA is emerged as an important tool (attributed to related biosensors) for investigating the DNA damage, and even to prepare electrode-bound DNA of small organic molecule ligands [16]. Figure 1.5 shows the electroactive groups in base pairs of adenine (A), guanine (G), cytosine (C), and thymine (T) structures.

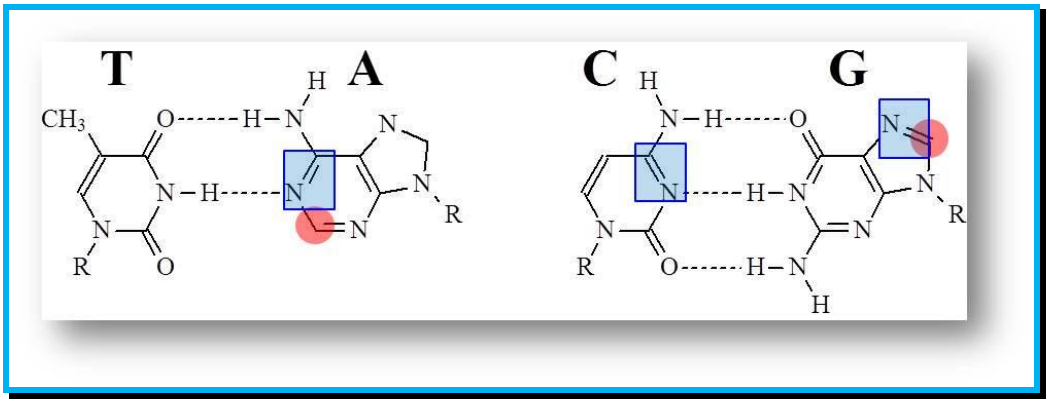

Figure 1.5: Electro Active Groups Present in Watson-Crick Base Pairs. The Primary Redox Sites Occurring in Base Pairs are shown in Circles (at mercury electrodes) and Rectangles (at carbon electrodes) [17]

In the present work, we describe synthesis and characterization of two newly designed perylene chromophoric derivatives (a perylene chromophoric diimide and a monoimide [PDI, PMI respectively]) for their potential applications in DNA binding studies (Figures 1.6 and 1.7). The photophysical characterization is carried out through UV and emission spectroscopic measurements. The synthesized materials are structurally proved through FTIR analysis.

Especially, the electrochemistry brought a new scope to explore the capability of perylene derivatives (through cyclic and squarewave voltammetry) to identify their potential interactions with DNA quadruplexes and for probable preparation of electrode-bound DNA of perylene derivatives. The DNA binding studies will be the future work of this project (Figure 1.8).

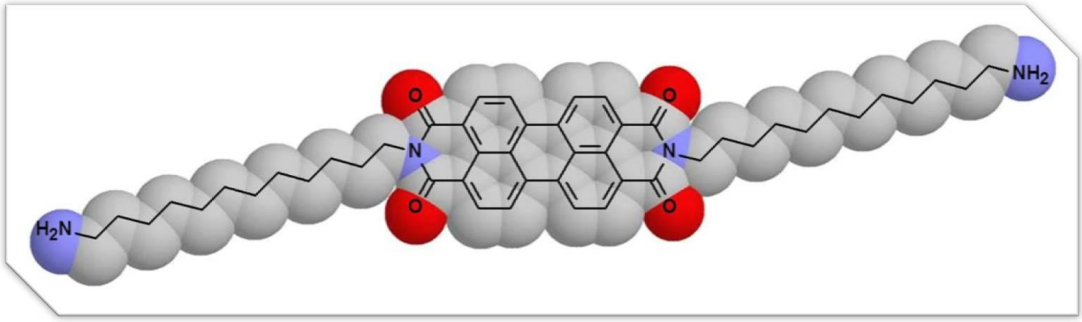

Figure 1.6: 3-D Structural Representation of the Synthesized Aminododecyl Perylene Diimide (ADPDI)

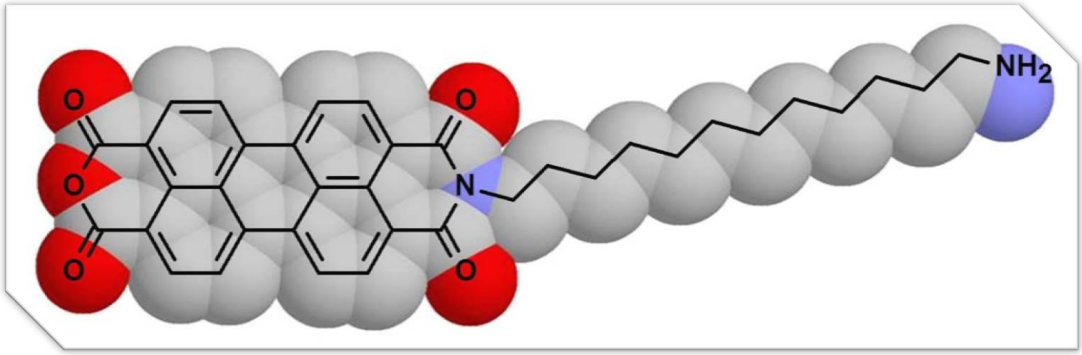

Figure 1.7: 3-D Structural Representation of the Synthesized Aminododecyl Perylene Monoimide (ADPMI)

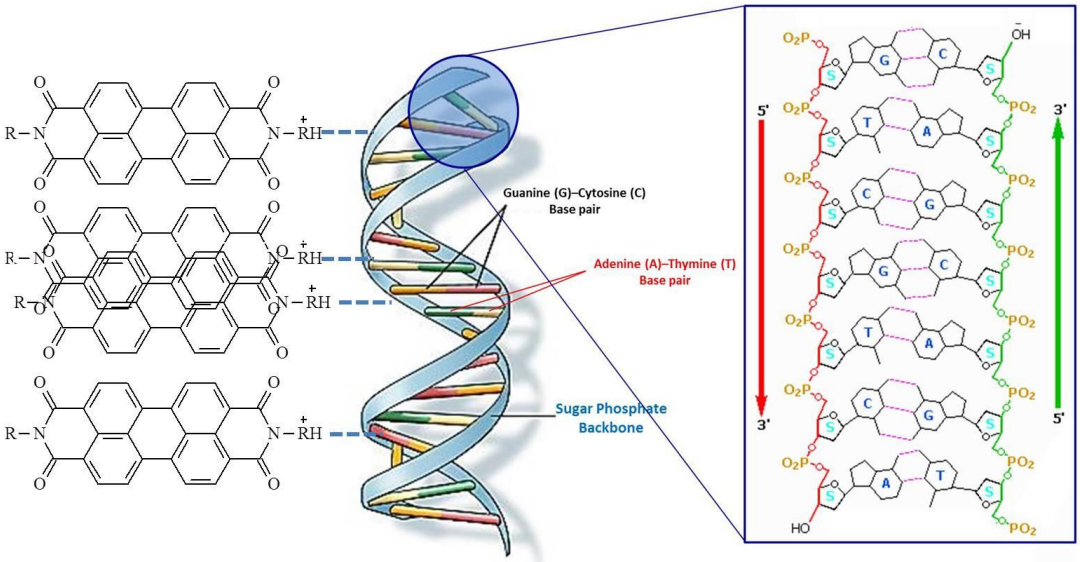

Figure 1.8: Representative Binding of Perylene Dyes to DNA

Chapter 2

THEORETICAL

2.1 Structural Characteristics of DNA

DNA (deoxyribonucleic acid) is a very important molecule in constructing wide novel organic, inorganic and metallic nanostructures. Although the applications of DNA are unlimited, it is important to make an overview on the structural characteristics of DNA which ultimately providing it such a remarkability (briefly explained in Figure 2.1).

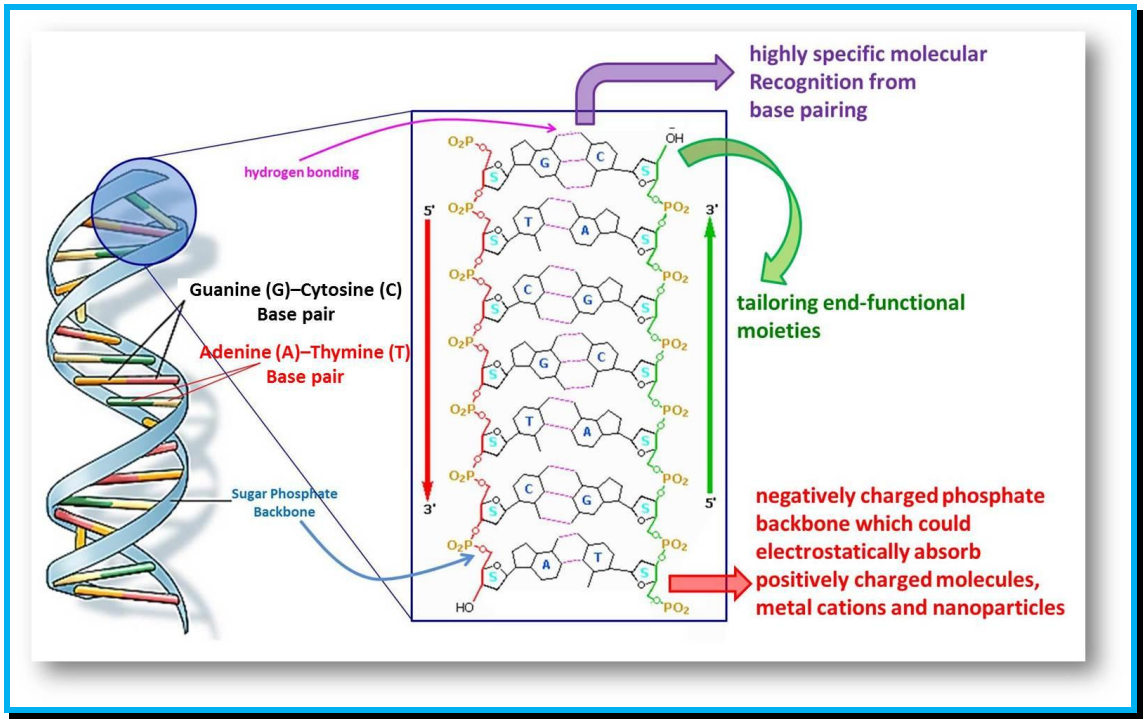

Figure 2.1: DNA Model (left) and its Structural Details (right)

As can be seen from Figure 2.1, it is very well known that DNA is mainly comprised of nucleotides. Nucleotides are smaller molecules and they are primarily composed of (1) a nitrogenous base (i.e., nitrogen-containing base); (2) a deoxyribose (sugar molecule based on carbon); and (3) a phosphate group (containing phosphate) which are attached to the sugar molecules. Adenine-A, thymine-T, guanine-G, and cytosine-C are the four basic types of nucleotides. The series of nucleotides as a polynucleotide DNA offers several structural advantages such as modifications at the end-functional groups and possibility for attraction and binding of positively charged entities (for example, metal cations, organic molecules bearing positive charged atoms, and nanoparticles, etc.) at its negatively charged backbone [18].

2.1.1 Structural Characteristics of Quadruplex Structures

Quadruplexes are the sequences of nucleic acids and contain guanine bases. They are usually referred as G-quadruplexes. As seen earlier in Figure 1.3, they are also called as G-tetrads or G_4–DNA as the guanine bases are associated through eight Hoogsteen guanine base-pair hydrogen bonding resulting in a square planar G-tetrad structure. G-quadruplex is formed when two or more of these G-tetrads are stacked over each other as shown in Figure 2.2. Most importantly, the G-quadruplex is additionally stabilized by placing a monovalent cation (exclusively potassium) at the central channel between each base pair of G-tetrads (Figure 2.2).

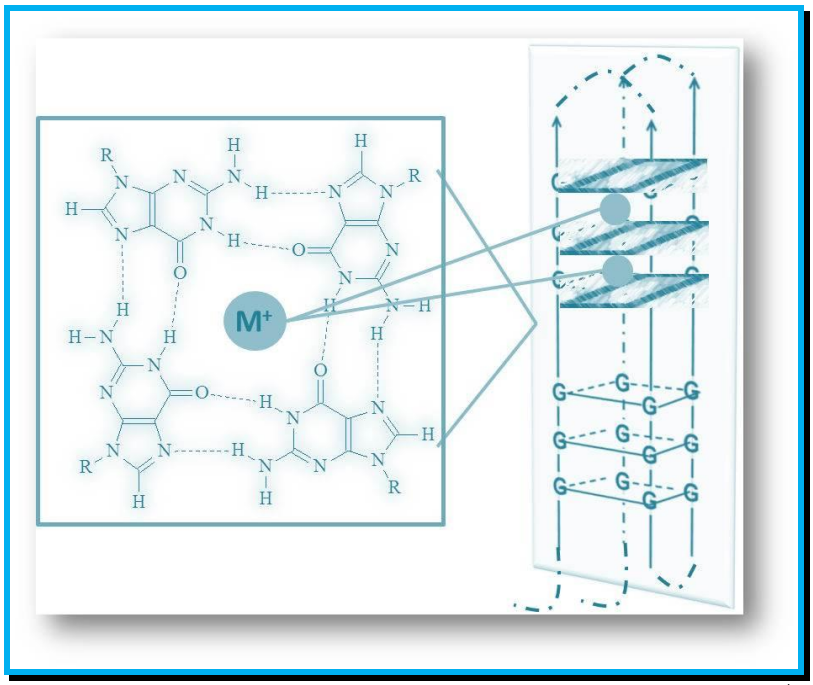

Figure 2.2: Stabilization of G-quadruplex by Monovalent Cation (M^+) and its Antiparallel Unimolecular Stacked Structure (right) with Three G-tetrads

These G-quadruplexes can be unimolecular, bimolecular or tetramolecular which rely on the number as well as orientation of the DNA strands and might arise (for a better approximation) from duplex DNA inside cells. The stabilization of G-quadruplexes by various ligands potentially stabilize the telomeric DNA, consequently telomerase inhibition would occur [10, 11, 19].

When guanine-rich nucleotides are chemically altered, it leads to probable polymorphism in G-quadruplexes and which might address its thermodynamically stabilized configurations. They can be intra- or inter- molecular and exhibit vast variety of topologies. There are so many important factors that affect the polymorphism/topology and self-assembly of G-quadruplexes such as the concentration and type of the monovalent cation, the concentration of DNA, and the existence of organic solvents [19].

2.2 Potential π-Conjugated Molecules for DNA Sequence Binding

It is obvious that alterations of DNA sequences (at the terminus of guanine-rich oligonucleotides) by attaching organic aromatic molecules covalently cause significant differences from their original counterpart sequences. The major change noticed is the increase in thermodynamic stability due to the π–π stacking abilities of aromatic chromophores which in turn protects the hydrogen bonds of nucleotides that present at terminal positions. There are numerous π–conjugated molecules which are binded to DNA for drug designing applications . In addition, various large organic chromophores (for example, 4,4′-dimethoxytrityl and *tert*-butyldiphenylsilyl, etc) were also reported which were attached covalently to tetramolecular G-quadruplexes [19].

2.2.1 Selective Ligands for G-Quadruplex Sturctures

Most of the active ligands and compounds induced to G-Quadruplex sturctures *via* binding are to inhibit telomerase. The ligands are based on the structures of porphyrins, anthraquinones, and derivatives of perylene, acridine, and dibenzophenanthroline, *etc* (Figure 2.3) [13].

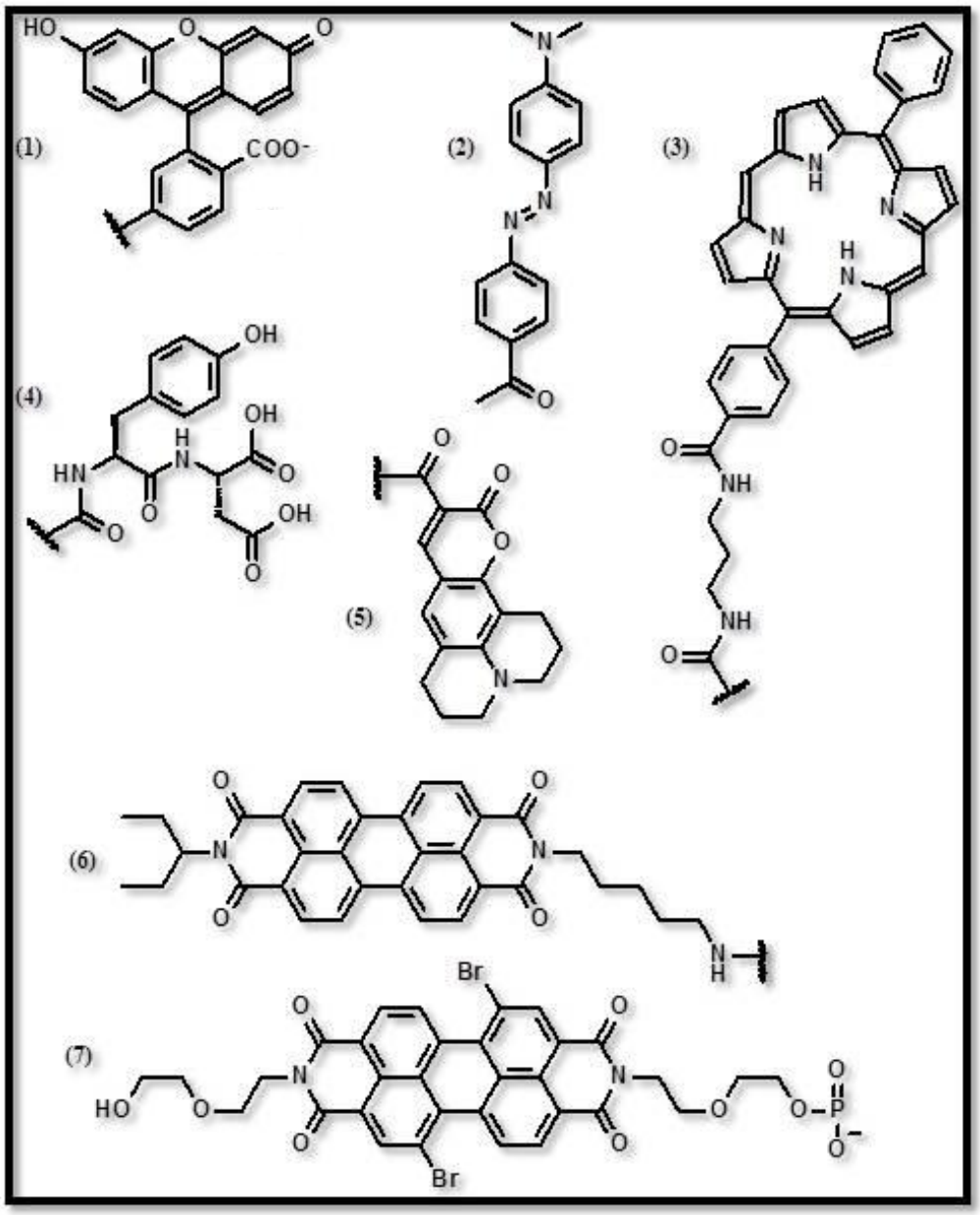

Figure 2.3: Aromatic π–conjugated molecules and Various Amino Acids Self-assembled as G-quadruplex Structures (molecules from 1–5); Organic Aromatic Ligands that can Change the Topology of G-quadruplex Structures (molecules 6, 7)

2.3 An Overview on Structural Properties of Perylene Chromophoric Derivatives

Perylene chromophoric dyes are excellent compounds and are very superior with versatile applications in many fields. The structural properties and advantages were briefly shown in Figure 1.2. The key point is their aromatic structure with conjugate double bonds and multiple carboxyl groups which offer versatile properties [20]. The conjugate aromatic rigid structure offers stability (thermal, electrochemical, and mechanical) and absorbs strongly the electromagnetic radiation [21]. The substitution at multiple positions (*see* Figure 1.2) offers versatile electronic properties. The perylene chromophoric dyes usually exhibit intense emission properties and deliver emission above 500 nm ranging to 800 nm. Hence, these dyes are also used as fluorescent markers and are widely applied in labelling applications. Interestingly, the perylene dyes usually undergo photoinduced electronic energy and electron transfer processes depending on the substituents attached at various positions of the perylene chromophore [22, 23]. These charge transfer and energy transfer properties could be explored *via* optical (photophysical) and electrochemical characterization (through UV-vis and fluorescence spectroscopy; cyclic and squarewave voltammetric measurements) [22].

One of the most useful points among many structural advantages of perylene derivatives is the strong electron accepting capacity due to the presence of four carbonyl groups. Furthermore, there is a chance of introducing positively charged substituents at the imide positions which are potential candidates for binding to DNA (for example, *see* Figure 1.4) and for forming G-quadruplex structures.

2.3.1 Important Properties of Perylene Dyes

Electrochemical properties of perylene chromophoric dyes are very important concerning the DNA binding studies as they are excellent electron acceptors and can be reduced easily at the carbonyl groups. Upon reduction, the perylene dyes generally form monovalent anion and respective dianion. The compounds usually exhibit electrochemical stability and reversibility [22]. The electronic properties are tunable with substitution of suitable moieties at the bay region of perylene chromophore. The core substitution of perylene chromophore has a great impact on the electronic nature of perylene derivative dyes. The imide substitutions also offer versatile electronic properties and are strictly related to the type of the moieties that are introduced. Perylene dyes are thus prepared according to the necessity and type of application by modifying the core- and imide- positions and the resulting perylene chromophoric dyes act as both electron donors and acceptors, respectively [5]. Electron donating perylene derivative dyes also show strong oxidation properties. Usually the HOMO (highest occupied molecular orbital), LUMO (lowest unoccupied molecular orbital), and band gap energies (E_g) are estimated to characterize the redox behaviour of perylene dyes both optically and electrochemically in solution and solid-state. These HOMO, LUMO and E_g values give absolute energetic positions. Generally, the perylene dyes exhibit diffusion-controlled charge transfer processes by obeying Stern–Volmer kinetics. It can be summarized that the perylene dyes are generally electroactive species with strong redox properties. The electronic properties of perylene dyes are therefore widely utilized and employed in electronic industry to prepare versatile optoelectronic devices [22].

Electrochemical Approach of Binding Perylene Derivatives to DNA

As seen earlier, there are active electroactive base pairs that constitute DNA (*see* Figure 1.5) and thus DNA has been analyzed primarily by voltammetric techniques and found that it is electroactive and show response at liquid mercury and solid carbon electrodes. Utilizing this feature, the researchers have prepared DNA-modified electrodes especially for the purpose of DNA based biosensors. Therefore, various perylene chromophoric-based modified DNA could be electrochemically bound to result in perylene derivative-based electrode bound DNA for sensing applications [16].

2.3.2 Interactions of G-Quadruplex/Perylene Derivative Ligands

There were so many perylene derivative dyes reported in literature which selectively bound to G-quadruplex DNA. In addition, the perylene chromophoric dyes offer another advantage of being capable of preparing conjugates with various materials. These conjugates were also successfully bound to DNA and the results were described in literature [24-29].

The ultimate approach of positively charged or hydrogen bond induced perylene derivative dye ligands that are bound to DNA is stabilization of the G-quadruplexes *via* external stacking to G-tetrads. As shown in Figures 2.1 and 2.2, the positively charged perylene dye interacts with the central cavity of G-tetrad and forms stacked structure on the 3′-terminal surface of a G -tetrad and stabilizes presumably tetramolecular parallel G -quadruplex. The incorporation could be also at 5′-terminal surface which may lead to the alteration of the guanine-rich oligonucleotides [27-29]. Therefore, the perylene dyes must enhance the non-covalent stacking interactions with G-quadruplexes. Perylene dyes can form aggregates and dimers in solutions and

these can promote parallel, two-molecular composition of G-quadruplex structure at both 5′-terminal ends that are established at the same side of the G-quadruplex structure [19].

2.3.3 Structural Design of Perylene Chromophoric Derivatives for DNA-Binding

It is very well known that DNA backbone is negatively charged due to the attached phosphate groups. Therefore there is an extra care required in designing the perylene chromophoric based ligands which can stabilize G-quadruplexes by selective binding to DNA (summarized in Figure 2.4).

Favoring the Stacking Interactions

First of all, the aromatic conjugated core of perylene dyes must be protected and could be enhanced if required by attaching various aromatic π-conjugated groups at various positions of the perylene chromophore. This can result in enhancement of various non-covalent interactions (for example, π–π interactions and hydrogen bonding) with G-tetrads and DNA grooves in order to stabilize G-quadruplexes (*via*. threading intercalation model) [8, 12]. In addition, the solubility of the perylene derivatives in aqueous solutions must be taken into account in order to enhance the stacking and assembling interactions.

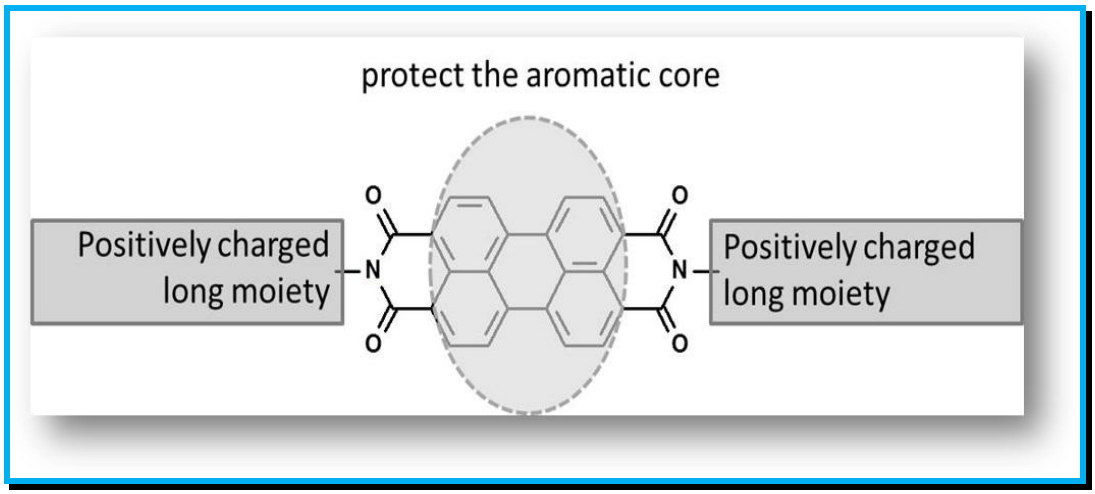

Figure 2.4: Summary of the Aspects in Designing Perylene Derivative Dyes for G-quadruplexes

Basic Side Chains

The designed perylene derivative dyes should stabilize the electrostatic interactions with the negatively charged DNA phosphates. This is more possible when the side chains attached at the imide positions should possess cationic moieties. It is very important to protect the electron-deficient chromophoric system as well as to contain the positive charge bearing side chain moieties (Figure 2.4). The integration in such a way of perylene chromophoric design not only enhances the formation and stabilization of G-quadruplexes but also plays key role in selecting its topology. In addition, such designs are capable of inhibiting telomerase efficiently. Another important factor concerning the side chain design at imide positions of perylene chromophore is that the dyes should have long distance between the positive charge bearing nitrogen atom and the aromatic moiety. This might result in inducing dimeric G-quadruplexes efficiently as well as increase in self-association in aqueous solutions [8, 12].

Chapter 3

EXPERIMENTAL

3.1 Materials and Instruments

The chemical reagents and solvents used in this work were purchased from Aldrich and were used without further purification unless otherwise mentioned. Few solvents were distilled according to the necessity by general distillation methods. Dried solvents are prepared by activating the molecular sieves (4 $\overset{o}{A}$) at 500 ^{o}C in a furnace and by keeping the solvent overnight in presence of activated sieves.

Spectroscopic graded solvents are used for spectroscopic analyses and the solvents are bubbled by purging inert gas for a short period of time before the analysis.

Analyte and KBr prepared pellets (press method) for FTIR spectrum by JASCO FT-IR spectrophotometer, solution absorption spectra of analytes and synthesized compounds by UV spectrophotometer (Varian-Cary-100), Emission spectra in solutions of analytes and synthesized compounds by Varian-Cary-Eclipse fluorescence were performed for detailed characterization.

3.2 Methods of Synthesis

The method of synthesis of perylene chromophoric dyes is widely reported in many research papers [1–5]. The method that was reported by Icil and co-workers is one of the most successful methods as it was confessing the high yields [2–5, 20–23]. The perylene chromophoric derivatives in the present work (ADPDI and ADPMI) are synthesized by the method reported by Icil and co-workers. The overall synthesis of the compounds is schematically shown in Scheme 3.1.

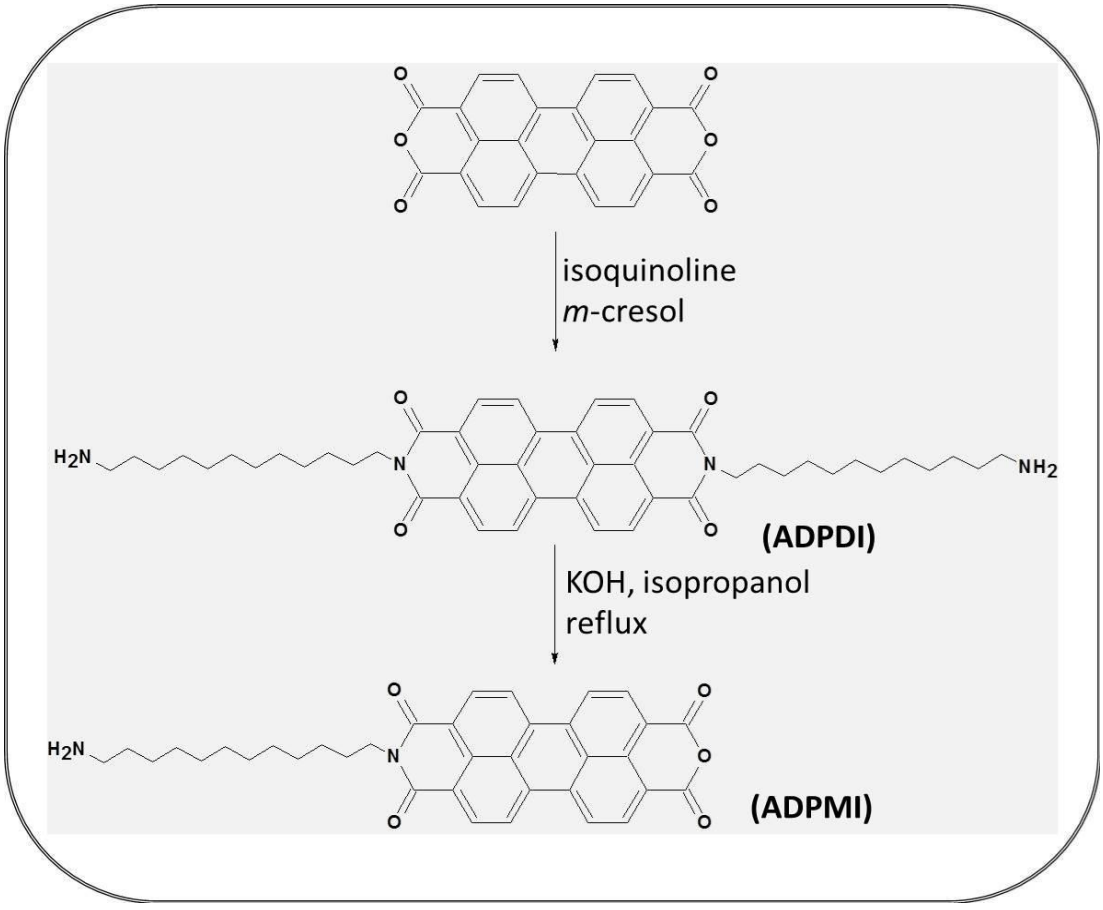

Scheme 3.1: Synthesis of Perylene Chromophoric Diimide and Monoimide Dyes (ADPDI and ADPMI, respectively)

PART-I: Synthesis of Aminododecyl Perylene Diimide, ADPDI

The synthesis of aminododecyl perylene diimide was carried out in a single step using the commercial starting material perylene dianhydride and commercial dodecyl amine. The synthesis scheme is shown below (Scheme 3.2), [30].

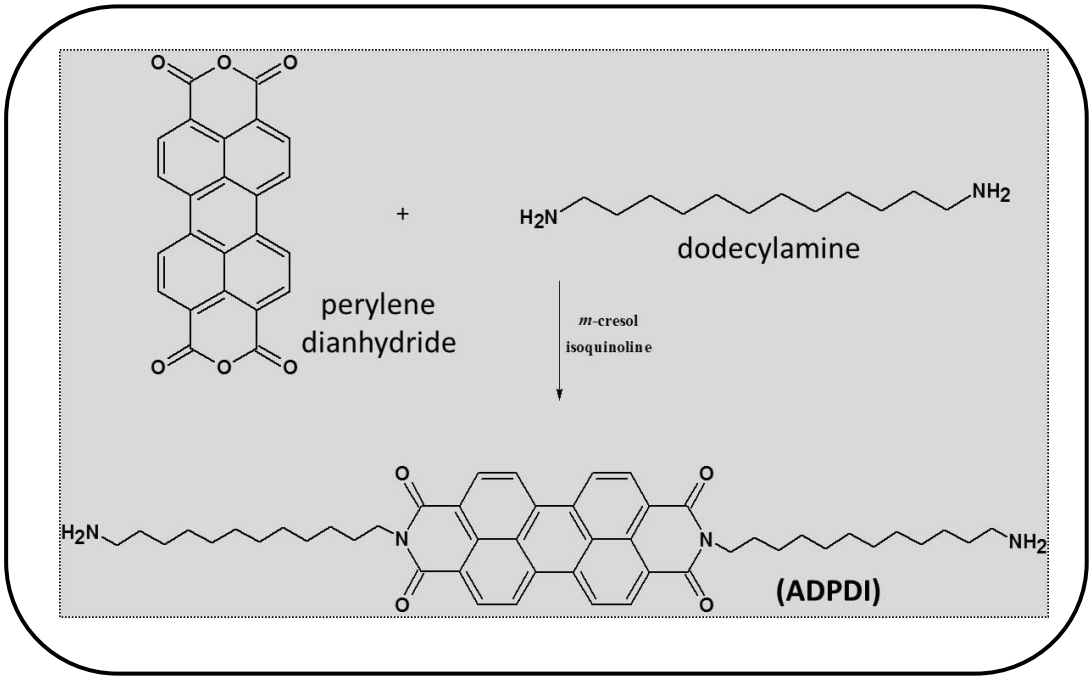

Scheme 3.2: Synthesis of N,N′-Bis(12-aminododecyl)-3,4,9,10-perylenebis-(dicarboximide), ADPDI [30]

PART-II: Synthesis of Aminododecyl Perylene Monoimide, ADPMI

The synthesis of aminododecyl perylene monoimide was carried out in a single step by refluxing the previous product of perylene diimide (ADPDI) in KOH, and isopropanol mixture (Scheme 3.3).

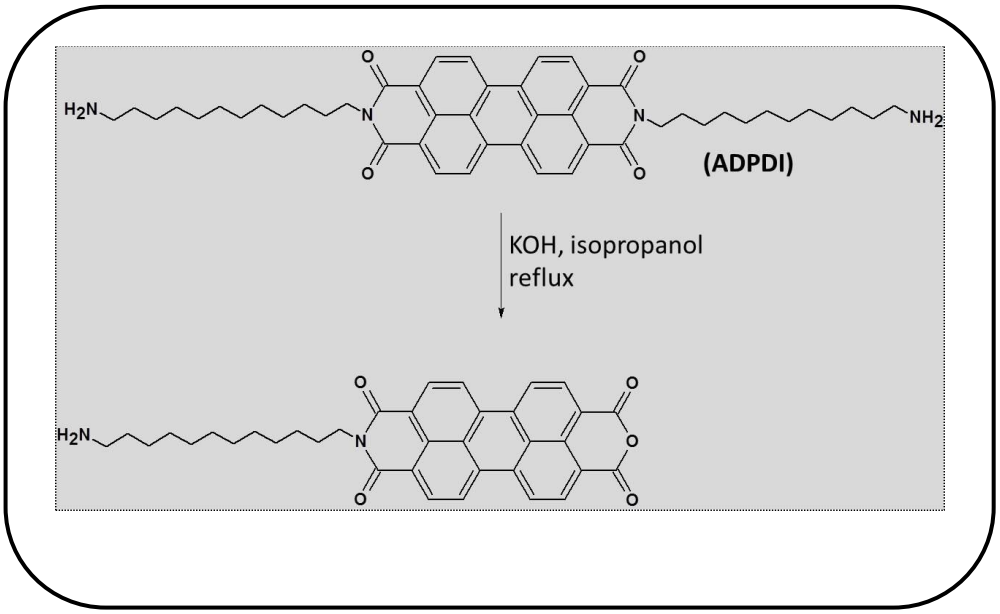

Scheme 3.3: Synthesis of N-(12-aminododecyl)-3,4,9,10-perylene- tetracarboxylic-3,4-anhydride-9,10-imide, ADPMI

3.3 Synthesis of N,N′-Bis (12-aminododecyl)-3,4,9,10-perylenebis-(dicarboximide) (ADPDI)

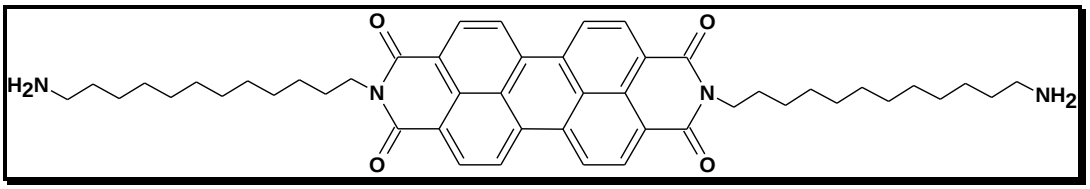

Three-necked balloon is pumped argon gas and provided a mixture of diaminododecane (1.28 g, 6.38 mmol) in a mixture of *m*-cresol (40 mL) and isoquinoline (4 mL). The mixture is stirred under argon gas for 30 min. Perylene 3,4,9,10-tetracarboxylic dianhydride (1 g, 2.55 mmol) is added and stirred at room temperature for 30 min. The mixture is heated at 80 ^{o}C for 2 h, at 120 ^{o}C for 2 h, at 150 ^{o}C for 4 h, at 180 ^{o}C for 8 h, and finally at 200 ^{o}C for 5 h. The reaction completion is confirmed by thin layer chromatography (TLC) and FTIR spectrum. The crude reaction mixture is now poured into acetone and the resulting precipitate is filtered. The filtrate is purified by applying it into an alcoholic solvent (ethanol) Soxhlet and dried in vacuum oven overnight to get pure aminododecyl perylene diimide dye [30].

Yield: 84% (1.62 g).

mp: >300 ^{o}C.

FT-IR (KBr, cm^{-1}): ν = 3304, 3059, 2922, 2850, 1696, 1655, 1596, 1579, 1342, 809, 746.

UV-Vis (DMF) (λ_{max}, nm; (ε_{max}, L mol^{-1} cm^{-1})): 458 (10400), 500 (17000), 526 (22000).

Fluorescence, λ_{max} (DMF, nm): 535, 576, and 624 nm.

3.4 Synthesis of N-(12-aminododecyl)-3,4,9,10-perylene-tetracarboxylic-3,4-anhydride-9,10-imide (ADPMI)

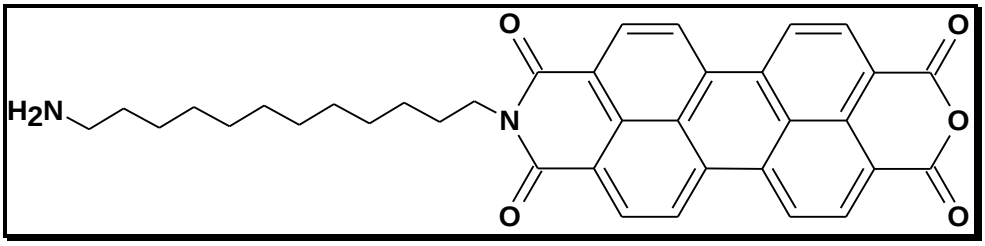

A two-necked balloon was added isopropanol (70 mL), water (30 mL), and KOH (3.7 g, 66 mmol) and stirred at room temperature for 30 min to obtain the homogeneous solution. Aminododecyl perylene diimide (ADPDI) was added to the mixture and refluxed for 24 h. The reaction mixture was poured into 100 mL dilute HCl. The resulting precipitate was filtered off and washed with distilled water. The crude product obtained was re-suspended in 5% KOH (100 mL) and stirred for 30 min at room temperature. The resulting precipitate was filtered off and again washed with dilute HCl. The final product obtained was applied to chloroform Soxhlet and dried under vacuum overnight to yield aminododecyl perylene monoimide (ADPMI).

Yield: 80% (0.6 g).

mp: >300 ^{o}C.

FT-IR (KBr, cm^{-1}): ν = 3404, 2926, 2854, 1777, 1730, 1696, 1652, 1595, 1092, 809, 468.

UV-Vis (DMF) (λ_{max}, nm; (ε_{max}, L mol^{-1} cm^{-1})): 455 (6100), 483 (12000), 519 (19000), 602 (10700).

Fluorescence, λ_{max} (DMF, nm): 534, 575, and 624 nm.

3.5 Proposed Reaction Mechanism for the General Synthesis of Perylene Diimide Dyes

Generally, the synthesis of perylene diimide dyes includes a four step reaction mechanism involving the main important nucleophilic attack and proton abstraction steps. The steps are outlined below.

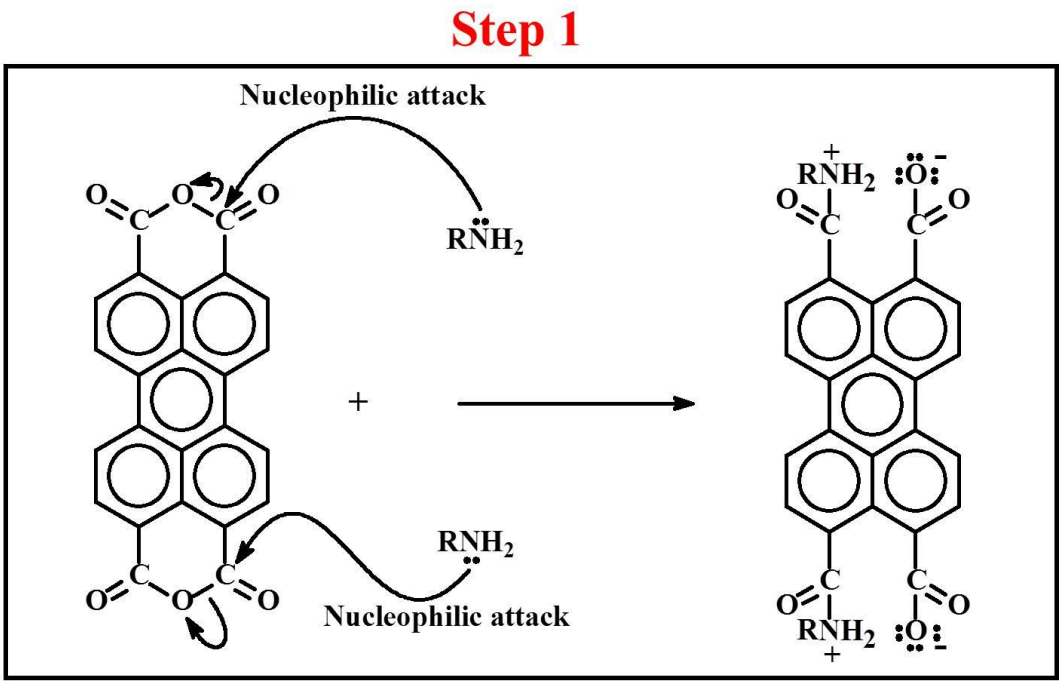

Step 2

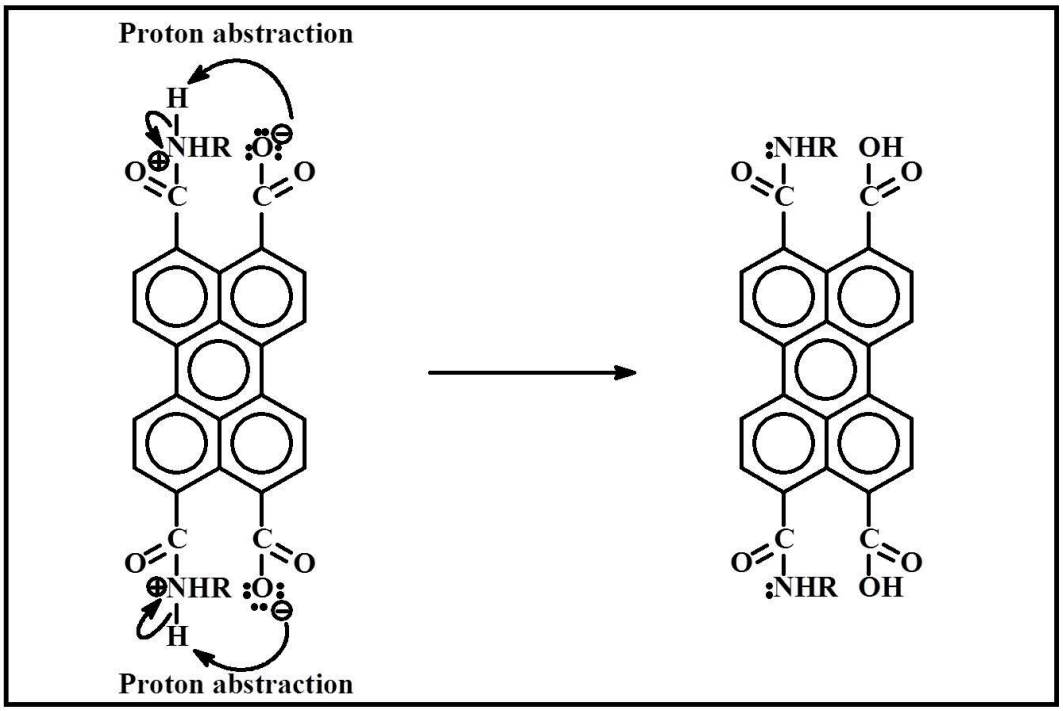
Proton abstraction
Proton abstraction

Step 3

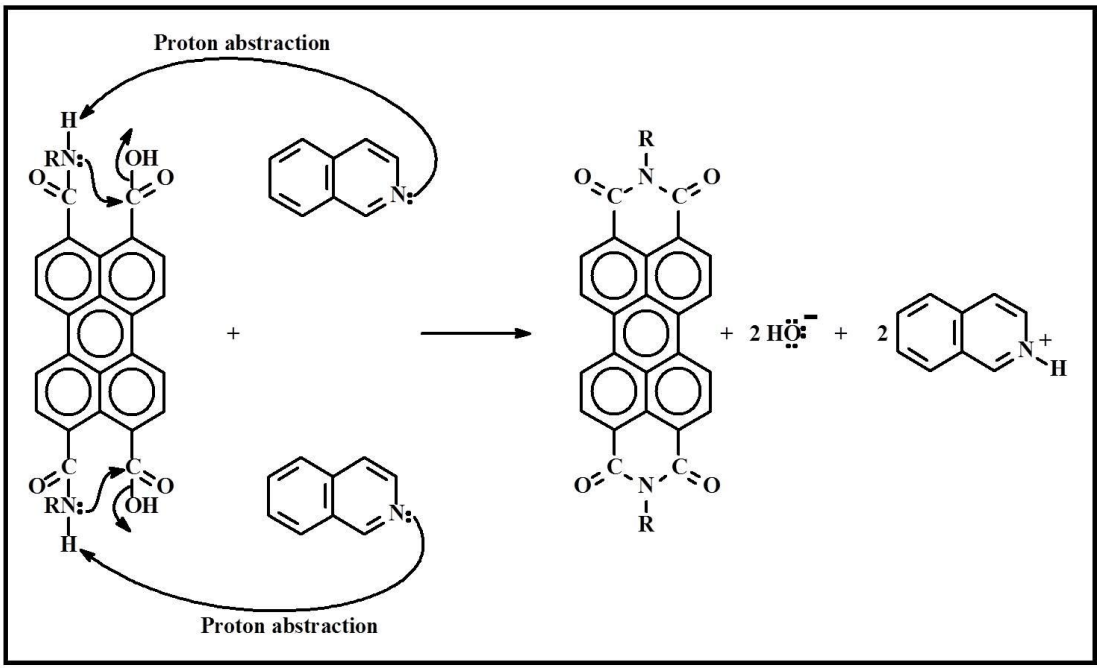
Proton abstraction
Proton abstraction

Step 4

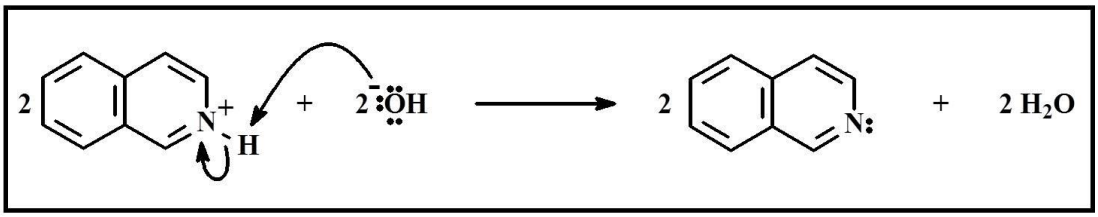

As seen from the four consecutive steps, reaction mechanism involves nucleophilic attack from the primary amine groups to form amide cation and carboxylate anion (step 1), proton abstraction to form amide and carboxylic acid (step 2), proton abstraction to serve ring closing and ring formation (step 3), and formation of isoquinoline back into the reaction (step 4).

Chapter 4

DATA AND CALCULATIONS

4.1 ε_{max} (Maximum Molar Absorption Coefficient) of Synthesized Compounds

The formula shown below (which is derived from Beer-Lamberts law) is used to estimate the ε_{max} (maximum molar absorption coefficient) value of synthesized ADPDI and ADPMI compounds.

$$\varepsilon_{max} = \frac{\mathbf{A}}{\mathbf{c}\boldsymbol{l}}$$

Where,

ε_{max} : Maximum molar absorption coefficient of the analyte in $M^{-1} \cdot cm^{-1}$ at λ_{max}

A : Absorbance value of the analyte at the wavelength of absorbance peak maximum

c : Concentration of the solution in $mol \cdot L^{-1}$

l : Path length that light travels through the solution in cm

Calculation of ε_{max} of ADPDI:

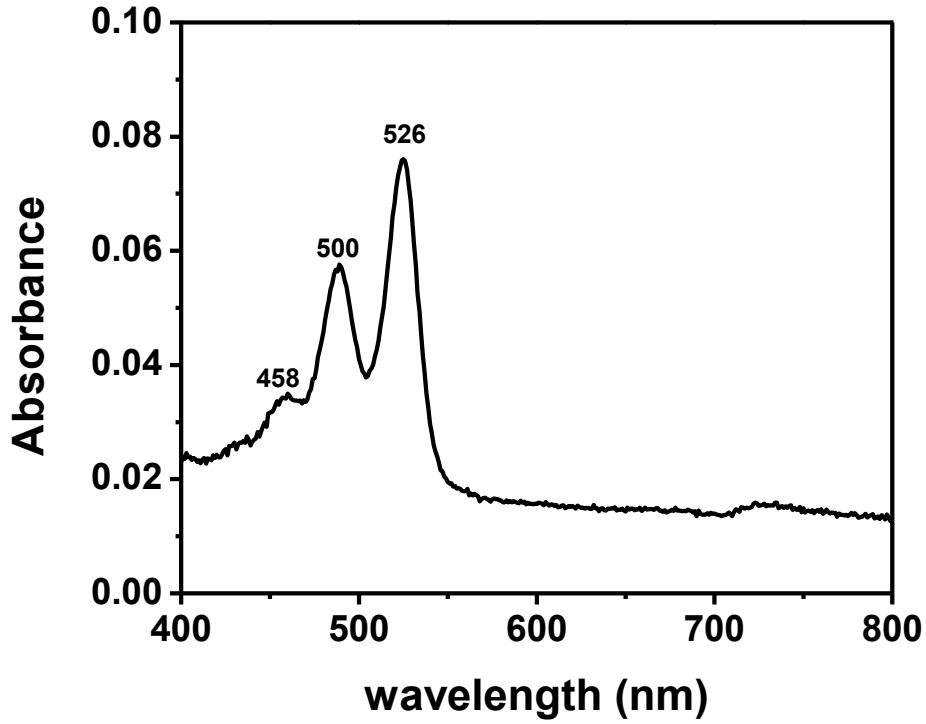

Figure 4.1: Absorption Spectrum of ADPDI in DMF at 3.45×10^{-6} M

According to the absorbance, concentration and wavelength data obtained from the absorption spectrum of ADPDI (Figure 4.1) in DMF, at peak maximum wavelength, λ_{max} = 526 nm the absorbance is 0.076 for concentration of $3.45\text{x}10^{-6}$ M.

$$\varepsilon_{max} = \frac{0.076}{3.45 \times 10^{-6}} = 22000\ \text{M}^{-1} \cdot \text{cm}^{-1}$$

ε_{max} of ADPDI in DMF = 22000 $\text{M}^{-1} \cdot \text{cm}^{-1}$

Similarly, the ε_{max} values of ADPDI for the absorption peaks at maximum wavelengths of 458 and 500 nm are 10400 and 17000 $\text{M}^{-1} \cdot \text{cm}^{-1}$, respectively.

The tables of absorbance data and corresponding ε_{max} values of synthesized ADPDI and ADPMI compounds at respective absorption wavelength peak maxima are listed below (Tables 4.1 and 4.2).

Table 4.1: Absorption Values of Synthesized ADPDI and ADPMI Compounds at Respective Absorption Wavelength Peak Maxima.

ADPDI	**$\lambda^{a}_{0\rightarrow2}$ = 458**	**$\lambda_{0\rightarrow1}$ = 500**	**$\lambda_{0\rightarrow0}$ = 526**	
A	0.036	0.059	0.076	
ADPMI	**$\lambda_{0\rightarrow2}$ = 455**	**$\lambda_{0\rightarrow1}$ = 483**	**$\lambda_{0\rightarrow0}$ = 519**	**$\lambda_{shoulder}$ = 602**
A	0.021	0.041	0.065	0.036

[a]λ value in the units of nm.

Table 4.2: ε_{max} Values of Synthesized ADPDI and ADPMI Compounds at Respective Absorption Wavelength Peak Maxima.

ADPDI	**$\lambda^{a}_{0\rightarrow2}$ = 458**	**$\lambda_{0\rightarrow1}$ = 500**	**$\lambda_{0\rightarrow0}$ = 526**	
ε_{max}[b]	10400	17000	22000	
ADPMI	**$\lambda_{0\rightarrow2}$ = 455**	**$\lambda_{0\rightarrow1}$ = 483**	**$\lambda_{0\rightarrow0}$ = 519**	**$\lambda_{shoulder}$ = 602**
ε_{max}	6100	12000	19000	10700

[a]λ value in the units of nm and [b]ε_{max} values in the units of $M^{-1} \cdot cm^{-1}$, respectively.

4.2 Φ_f (Fluorescence Quantum Yield) of Synthesized Compounds

Fluorescence quantum yield is a measure of the number of photons emitted to the number of photons absorbed by the analyte with respect to the reference compound whose fluorescence quantum yield is known previously.

The fluorescence quantum yields of the synthesized ADPDI and ADPMI compounds have been calculated from the following formula [2–5, 20–23, 30].

$$\Phi_u = \frac{A_{std}}{A_u} \times \frac{S_u}{S_{std}} \times \left(\frac{n_u}{n_{std}}\right)^2 \times \Phi_{std}$$

Where,

Φ_u: Fluorescence quantum yield of unknown compound

A_{std}: Absorbance of the reference compound at the excitation wavelength

A_u: Absorbance of the unknown compound at the excitation wavelength

S_{std}: The integrated emission area across the band of reference compound

S_u: The integrated emission area across the band of unknown compound

n_{std}: Refractive index of reference solvent

n_u: Refractive index of unknown solvent

Φ_{std}: Fluorescence quantum yield of reference compound

Φ_f Calculation of ADPDI in Chloroform

The reference is N,N′-bis(dodecyl)-3,4,9,10-perylenebis(discarboximide) [2–5, 30]

Φ_{std} = 1 in chloroform

A_{std} = 0.1055

A_u = 0.1012

S_u = 3304.86

S_{std} = 4129.22

$$\phi_f = \frac{0.1055}{0.1012} \times \frac{3304.86}{4129.22} \times 1$$

$\Phi_{f,ADPDI}$ = 0.83

Φ_f calculation of ADPMI in DMF

The reference is N,N′-bis(dodecyl)-3,4,9,10-perylenebis(discarboximide)

n_u = 1.431 for DMF

n_{std} = 1.446 for $CHCl_3$

Φ_{std} = 1 in chloroform

A_u = 0.098

S_u = 1538.94

A_{std} = 0.1055

S_{std} = 4129.22

$$\phi_f = \frac{0.1055}{0.0980} \times \frac{1538.94}{4129.22} \times \left(\frac{1.431}{1.446}\right)^2 \times 1$$

$\Phi_{f,\ ADPMI}$ = 0.39

4.3 FWHM (Full Width Half Maximum of Selected Absorption, $\Delta\bar{\upsilon}_{1/2}$) of Synthesized Compounds

The formula shown below is used to estimate the $\Delta\bar{\upsilon}_{1/2}$ (FWHM) of synthesized ADPDI and ADPMI compounds.

$$\Delta\bar{\upsilon}_{1/2} = \bar{\upsilon}_{I} - \bar{\upsilon}_{II}$$

Where,

$\Delta\bar{\upsilon}_{1/2}$: FWHM of selected absorption maximum in cm^{-1}

$\bar{\upsilon}_{I} - \bar{\upsilon}_{II}$: The estimated frequencies from the absorption of analyte in cm^{-1}

Calculation of $\Delta\bar{\upsilon}_{1/2}$ of ADPDI:

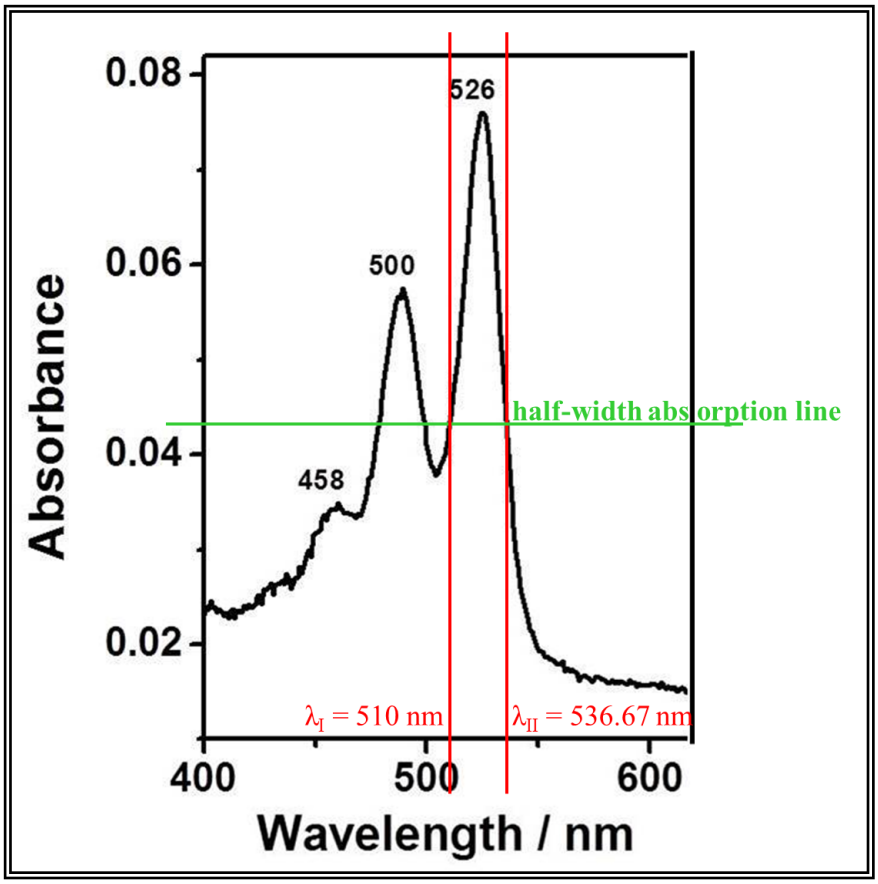

Figure 4.2: Estimation of FWHM from the Calculated Frequencies (Shown with Red Colored Lines) of Absorption Spectrum of ADPDI in DMF at 3.45×10^{-6} M

From Figure 4.2,

$\lambda_I =$ 510 nm

$\rightarrow \lambda_I = 510 \text{ nm} \times \frac{10^{-9} m}{1 nm} * \frac{1 cm}{10^{-2} m} = 510 \times 10^{-7} \text{ cm}$

$\rightarrow \bar{\upsilon}_I = \frac{1}{510 \times 10^{-7} \text{ cm}} = 19607.84 \text{ cm}^{-1}$

$\lambda_{II} =$ 536.67 nm

$\rightarrow \lambda_{II} = 536.67 \text{ nm} \times \frac{10^{-9} m}{1 nm} * \frac{1 cm}{10^{-2} m} = 536.67 \times 10^{-7} \text{ cm}$

$\rightarrow \bar{\upsilon}_{II} = \frac{1}{536.67 \times 10^{-7} \text{ cm}} = 18633.42 \text{ cm}^{-1}$

$\Delta\bar{\upsilon}_{1/2, ADPDI} = \bar{\upsilon}_I - \bar{\upsilon}_{II} = 19607.84 \text{ cm}^{-1} - 18633.42 \text{ cm}^{-1} = 974.42 \text{ cm}^{-1}$

$\rightarrow \Delta\bar{\upsilon}_{1/2, ADPDI} = 974.42 \text{ cm}^{-1}$

Based on the above method of calculation, FWHM values of synthesized compounds are calculated in different solvents for comparison and are listed in the following table (Table 4.3).

Table 4.3: FWHM ($\Delta\bar{\upsilon}_{1/2}$) Values of Synthesized ADPDI and ADPMI in Different Solvents.

ADPDI		
Solvent	**λ_I, λ_{II} (nm) / $\bar{\upsilon}_I$,$\bar{\upsilon}_{II}$ (cm^{-1})**	**$\Delta\bar{\upsilon}_{1/2, ADPDI}$ (cm^{-1})**
DMF	510, 536.67 / 19607.84, 18633.42	974.42
isoquinoline	520.27, 555.41 / 19220.79, 18004.72	1216.07
ADPMI		
Solvent	**λ_I, λ_{II} (nm) / $\bar{\upsilon}_I$,$\bar{\upsilon}_{II}$ (cm^{-1})**	**$\Delta\bar{\upsilon}_{1/2, ADPMI}$ (cm^{-1})**
DMF	504.55, 534.85 / 19819.64, 18696.83	1122.81
isoquinoline	505.55, 552.79 / 19780.44, 18090.05	1690.39
DMSO	501.61, 541.94 / 19935.81, 18452.23	1483.58

4.4 τ_0 (Theoretical Radiative Lifetime) of Synthesized Compounds

The formula shown below is used to estimate the τ_0 of synthesized ADPDI and ADPMI compounds [2–5, 20–23, 30].

$$\tau_0 = \frac{3.5*10^8}{\varepsilon_{max} * \bar{\upsilon}^2_{max} * \Delta\bar{\upsilon}_{1/2}}$$

Where,

τ_0 : Theoretical/Natural radiative lifetime in ns

$\bar{\upsilon}_{max}$: Mean frequency for the maximum absorption band in cm^{-1}

$\Delta\bar{\upsilon}_{1/2}$: FWHM of selected absorption maximum in cm^{-1}

ε_{max}: Maximum molar absorption coefficient of the analyte in $M^{-1} \cdot cm^{-1}$

Theoretical radiative lifetime of ADPDI:

λ_{max}= 526 nm in DMF, which is shown from Figures 4.1 and 4.2

ε_{max} = 22000 $M^{-1} \cdot cm^{-1}$

$\Delta\bar{\upsilon}_{1/2}$ = 974.42 cm^{-1}

$\lambda_{max} = 526\ nm * \frac{10^{-9} m}{1\ nm} * \frac{1\ cm}{10^{-2} m} = 526 \times 10^{-7}$ cm

$\rightarrow \bar{\upsilon}_{max} = \frac{1}{526 \times 10^{-7}\ cm} = 19011.41\ cm^{-1}$

$\rightarrow \bar{\upsilon}^2_{max} = (19011.41\ cm^{-1})^2 = 3.61 \times 10^8\ cm^{-2}$

$\rightarrow \tau_0 = \frac{3.5*10^8}{\varepsilon_{max} * \bar{\upsilon}^2_{max} * \Delta\bar{\upsilon}_{1/2}} = \frac{3.5 \times 10^8}{22000 \times 3.61 \times 10^8 \times 974.42}$

$\rightarrow \tau_0 = 4.52 \times 10^{-8}$ s

$\rightarrow \tau_0 = 45.2$ ns

According to the above method of calculation, τ_0 values of the synthesized compounds in various solvents are listed as follows (Table 4.4).

Table 4.4: τ_0 Data of ADPDI and ADPMI in Various Solvents.

ADPDI				
Solvent	λ_{max}**/nm**	$\varepsilon_{max}/M^{-1} \cdot cm^{-1}$	$\Delta\bar{\upsilon}_{1/2,\ ADPDI}$ **(cm^{-1})**	τ_0**/ns**
DMF	526	22000	974.42	45.2
isoquinoline	540	47000	1216.07	17.9
ADPMI				
Solvent	λ_{max}**/nm**	$\varepsilon_{max}/M^{-1} \cdot cm^{-1}$	$\Delta\bar{\upsilon}_{1/2,\ ADPMI}$ **(cm^{-1})**	τ_0**/ns**
DMF	519	19000	1122.81	44.2
isoquinoline	531	47000	1690.39	12.4
DMSO	522	45000	1483.58	14.3

4.5 Method of Calculation of Theoretical Fluorescence Lifetime (τ_f)

Theoretical Fluorescence Lifetime (τ_f) can be calculated from the following formula.

$$\boldsymbol{\tau_f = \tau_0 \times \Phi_f}$$

Accordingly, for ADPDI in DMF,

$\rightarrow$ τ_f = 45.2 ns $\times$ 0.83* = 37.5 ns

$\rightarrow$ $\boldsymbol{\tau_{f,\,ADPDI}}$ **= 37.5 ns**

*the solvent factor is omitted as Φ_f of ADPDI is measured in chloroform.

Accordingly, for ADPMI in DMF,

$\rightarrow$ τ_f = 44.2 ns $\times$ 0.39 = 17.2 ns

$\rightarrow$ $\boldsymbol{\tau_{f,\,ADPMI}}$ **= 17.2 ns**

4.6 k_f (Fluorescence Rate Constant) Values of Synthesized Compounds

The formula shown below is used to estimate the k_f of synthesized ADPDI and ADPMI compounds theoretically.

$$k_f = \frac{1}{\tau_0}$$

Where,

k_f : Fluorescence rate constant in s^{-1}

τ_0 : Theoretical radiative lifetime in s

Fluorescence rate constant values (k_f) of ADPDI:

$\rightarrow \quad k_f = \frac{1}{\tau_0}$

$\rightarrow \quad \frac{1}{4.52 \times 10^{-8}\ s} = 2.21 \times 10^7\ s^{-1}$

$\rightarrow \quad k_f = 2.21 \times 10^7\ s^{-1}$

In the similar method, the fluorescence rate constants were measured for both ADPDI and ADPMI in different solvents and the values were tabulated below (Table 4.5).

Table 4.5: k_f Data of ADPDI and ADPMI in Various Solvents.

ADPDI		
Solvent	τ_0/ns	k_f/s^{-1}
DMF	45.2	2.21×10^7
isoquinoline	17.9	5.59×10^7
ADPMI		
Solvent	τ_0/ns	k_f/s^{-1}
DMF	44.2	2.26×10^7
isoquinoline	12.4	8.06×10^7
DMSO	14.3	7.00×10^7

4.7 k_d (Rate Constants of Radiationless Deactivation) Values of Synthesized Compounds

The rate constants of radiationless deactivations of the compounds were calculated by the following equation.

$$k_d = \left(\frac{k_f}{\Phi_f}\right) - k_f$$

Where,

k_d: Rate constant of radiationless deactivation in s^{-1}

k_f: Fluorescence rate constant in s^{-1}

Φ_f: Fluorescence quantum yield

Rate Constant of Radiationless Deactivation of ADPDI in DMF:

⇨

$$\left(\frac{2.21\times 10^7\ s^{-1}}{0.83}\right) - 2.21\times 10^7\ s^{-1}$$

=> k_d, ADPDI* = $4.53 \times 10^6\ s^{-1}$

*the solvent factor is omitted as Φ_f of ADPDI is measured in chloroform.

The same method is applied in order to estimate the kd values of the synthesized ADPDI and ADPMI compounds in various solvents and the values are listed in the following table (Table 4.6).

Table 4.6: k_d Data of ADPDI and ADPMI in Various Solvents.

ADPDI			
Solvent	$\boldsymbol{\Phi_f}$	$\boldsymbol{k_f/s^{-1}}$	$\boldsymbol{k_d/s^{-1}}$
chloroform	0.83	2.21×10^7	4.53×10^6
ADPMI			
Solvent	$\boldsymbol{\Phi_f}$	$\boldsymbol{k_f/s^{-1}}$	$\boldsymbol{k_d/s^{-1}}$
DMF	0.39	2.26×10^7	3.53×10^7

4.8 *f* (Oscillator Strength) Values of Synthesized Compounds

Theoretically, the formula shown below is used to estimate the dimensionless quantity (*f*) of synthesized ADPDI and ADPMI compounds.

$$f = 4.32 * 10^{-9} \Delta\bar{\upsilon}_{1/2}\, \varepsilon_{max}$$

Where,

f : The value of oscillator strength

$\Delta\bar{\upsilon}_{1/2}$: FWHM of selected absorption maximum in cm^{-1}

ε_{max} : Maximum molar absorption coefficient of the analyte in $M^{-1} \cdot cm^{-1}$

The value of oscillator strength of ADPDI:

$\rightarrow f = 4.32 * 10^{-9} \Delta\bar{\upsilon}_{1/2}\, \varepsilon_{max}$

$\rightarrow f = 4.32 \times 10^{-9} \times 974.42 \times 22000 = 0.09$

$\rightarrow f_{ADPDI} = 0.09$

In the similar method, the strength of electronic transitions in terms of *f* values were measured for both ADPDI and ADPMI in different solvents and the values were tabulated below (Table 4.7).

Table 4.7: f Data of ADPDI and ADPMI in Various Solvents.

ADPDI			
Solvent	$\varepsilon_{max}/M^{-1} \cdot cm^{-1}$	$\Delta\bar{\upsilon}_{1/2,\ ADPDI}$ **(cm $^{-1}$)**	f
DMF	22000	974.42	0.08
isoquinoline	47000	1216.07	0.25
ADPMI			
Solvent	$\varepsilon_{max}/M^{-1} \cdot cm^{-1}$	$\Delta\bar{\upsilon}_{1/2,\ ADPMI}$ **(cm $^{-1}$)**	f
DMF	19000	1122.81	0.09
isoquinoline	47000	1690.39	0.34
DMSO	45000	1483.58	0.29

4.9 E_s (Singlet Energy) Values of Synthesized Compounds

Theoretically, the formula shown below is used to estimate the energy required for electronic transition from ground to excited states (E_s) of synthesized ADPDI and ADPMI compounds.

$$E_s = \frac{2.86 * 10^5}{\lambda_{max}}$$

Where,

E_s: The singlet energy in (kcal·mol $^{-1}$)

λ_{max}: The maximum absorption wavelength in Å

The E_s value of ADPDI:

$$\rightarrow E_s = \frac{2.86*10^5}{\lambda_{max}} = \frac{2.86 \times 10^5}{5260} = 54.37 \text{ kcal·mol}^{-1}$$

$\rightarrow E_s = 54.37$ kcal·mol $^{-1}$

According to the above method of calculation, the energy required for electronic transitions in terms of E_s values were measured for both ADPDI and ADPMI in different solvents and the values were tabulated below (Table 4.8).

Table 4.8: E_s Data of ADPDI and ADPMI in Various Solvents.

ADPDI		
Solvent	**λ_{max}/nm**	**$E_{s,\ ADPDI}$ (kcal·mol^{-1})**
DMF	526	54.37
isoquinoline	540	52.57
ADPMI		
Solvent	**λ_{max}/nm**	**$E_{s,\ ADPMI}$ (kcal·mol^{-1})**
DMF	519	55.11
isoquinoline	531	53.86
DMSO	522	54.79

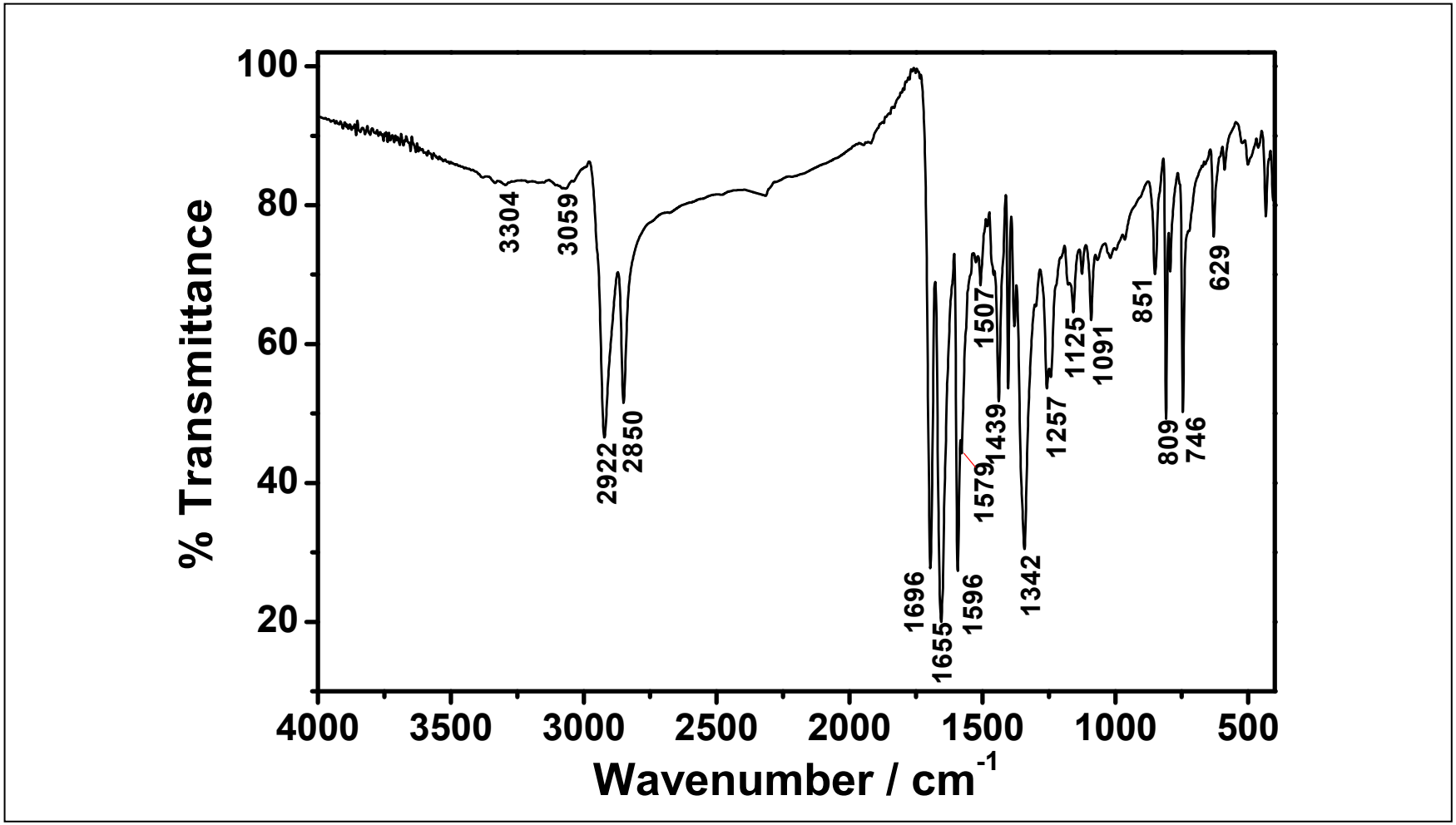

Figure 4.3: FTIR Spectrum of ADPDI

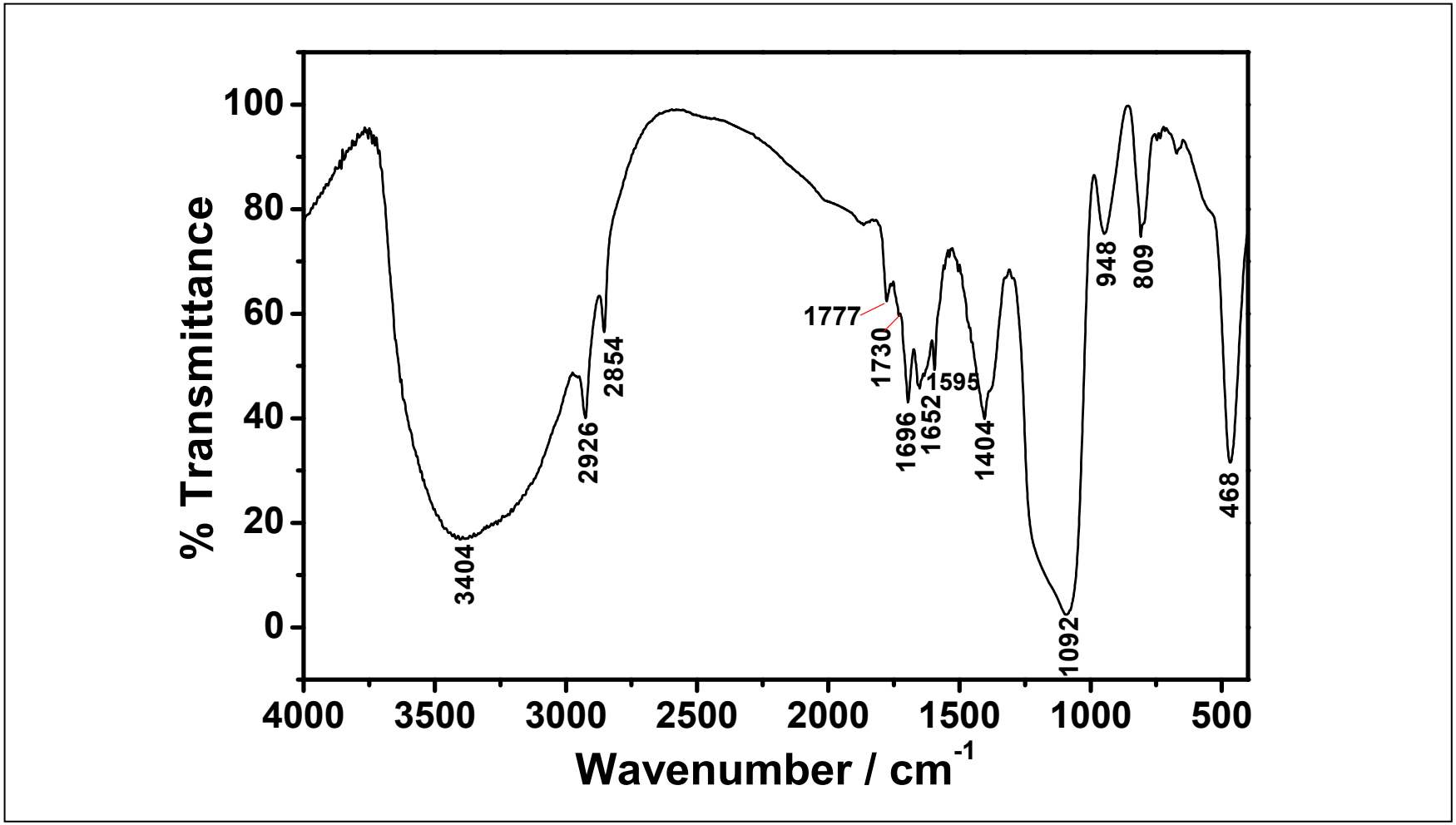

Figure 4.4: FTIR Spectrum of ADPMI

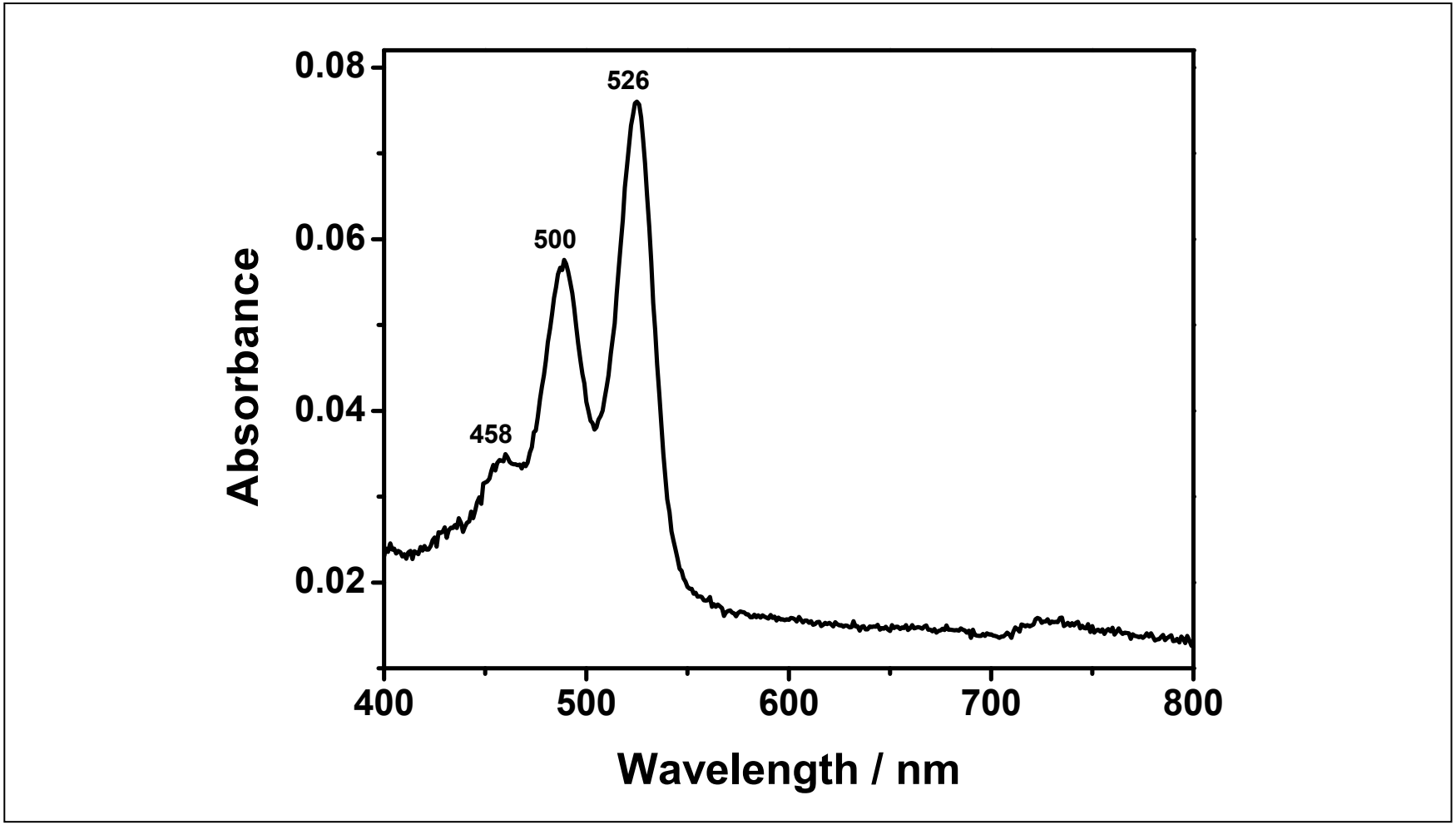

Figure 4.5: Absorbance Spectrum of ADPDI in DMF

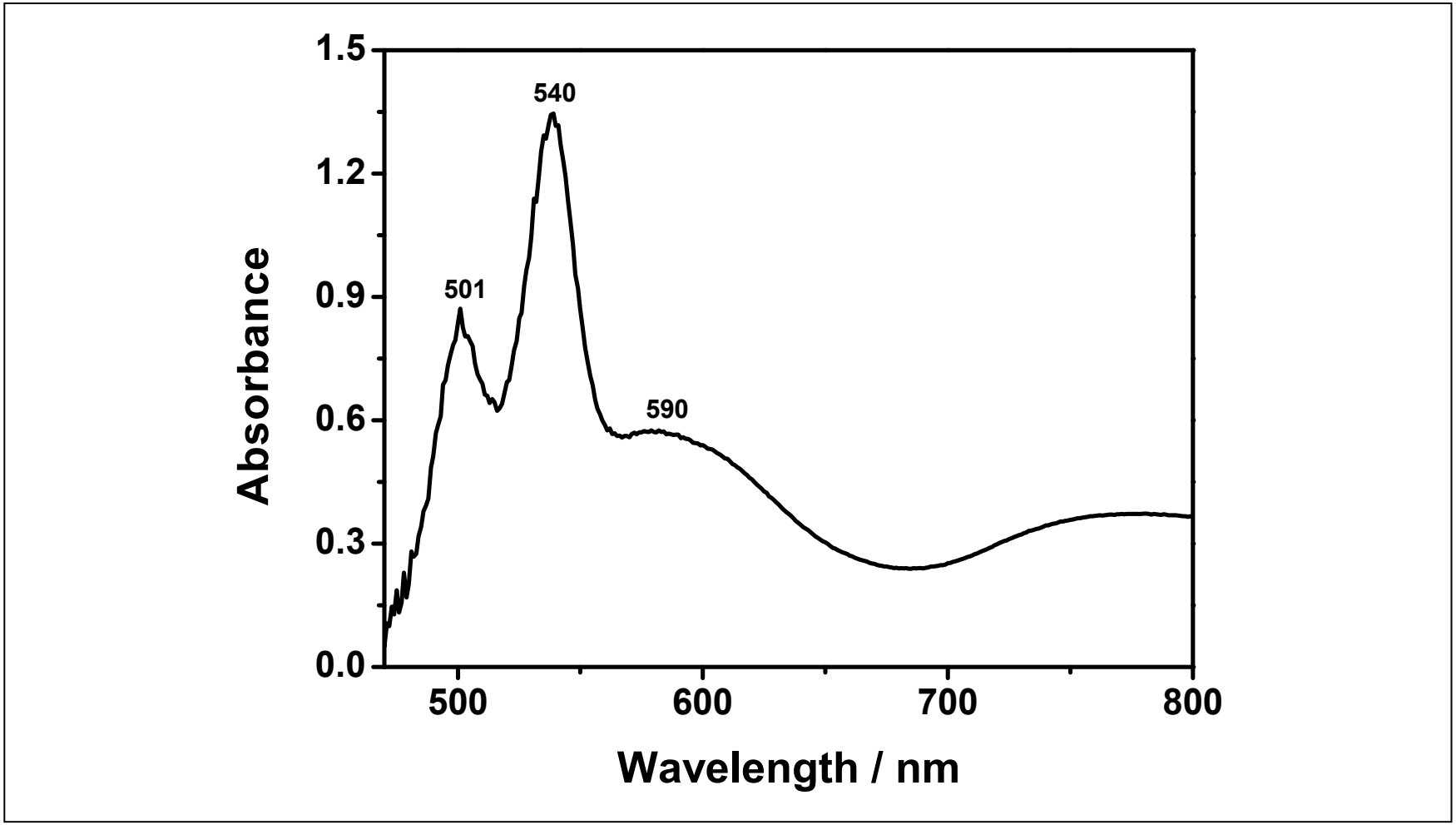

Figure 4.6: Absorbance Spectrum of ADPDI in Isoquinoline

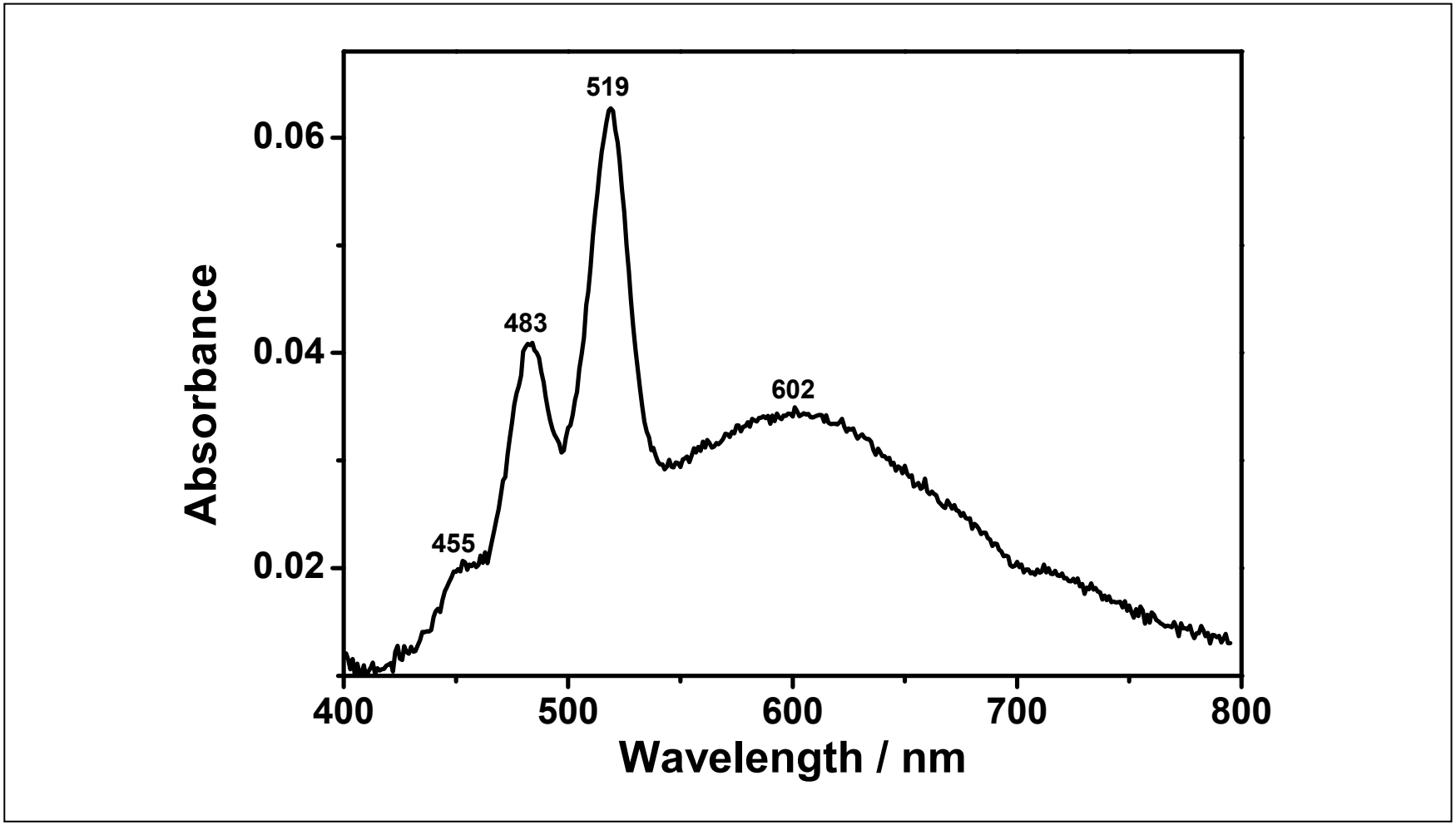

Figure 4.7: Absorbance Spectrum of ADPMI in DMF

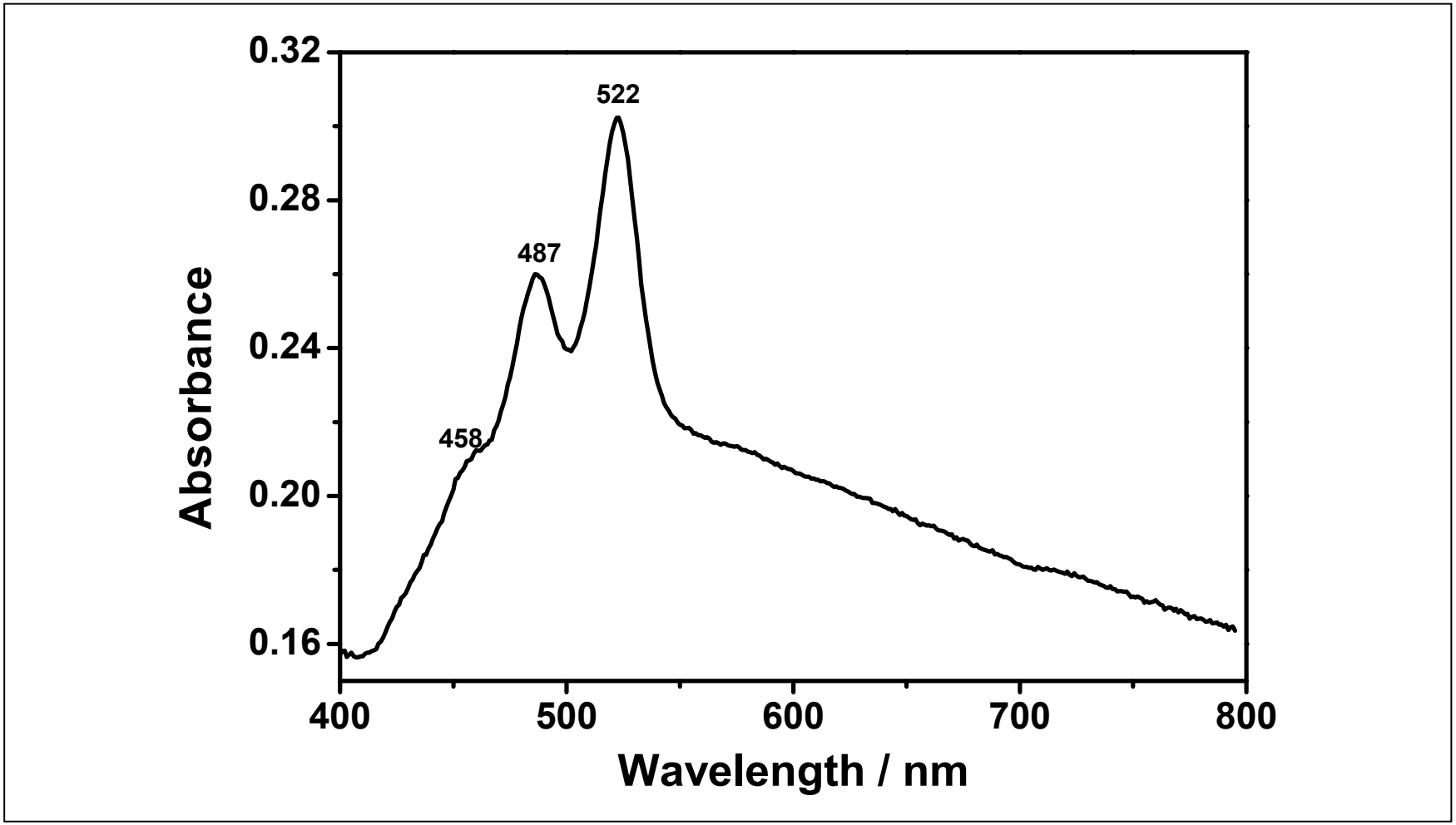

Figure 4.8: Absorbance Spectrum of ADPMI in DMSO

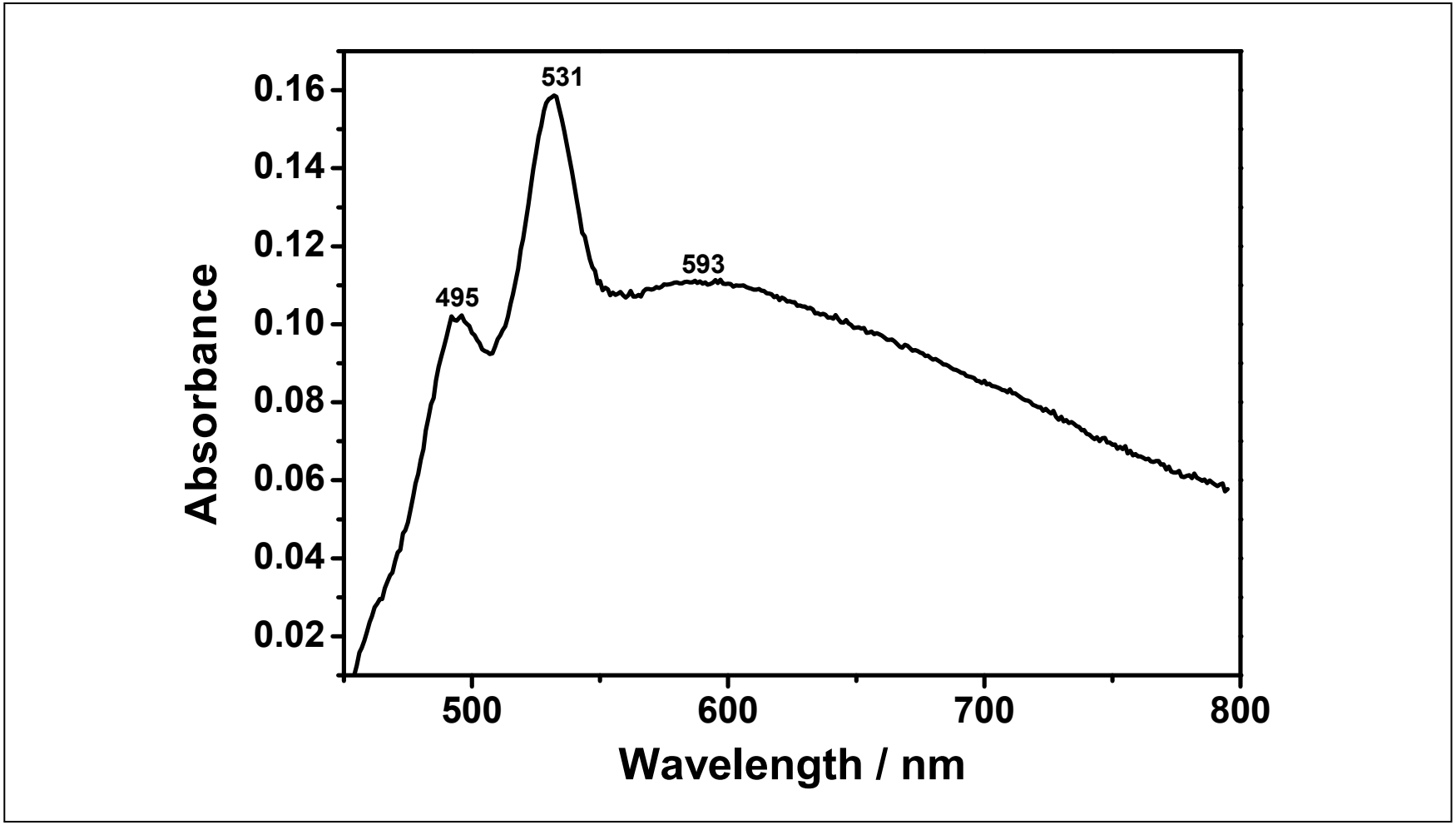

Figure 4.9: Absorbance Spectrum of ADPMI in Isoquinoline

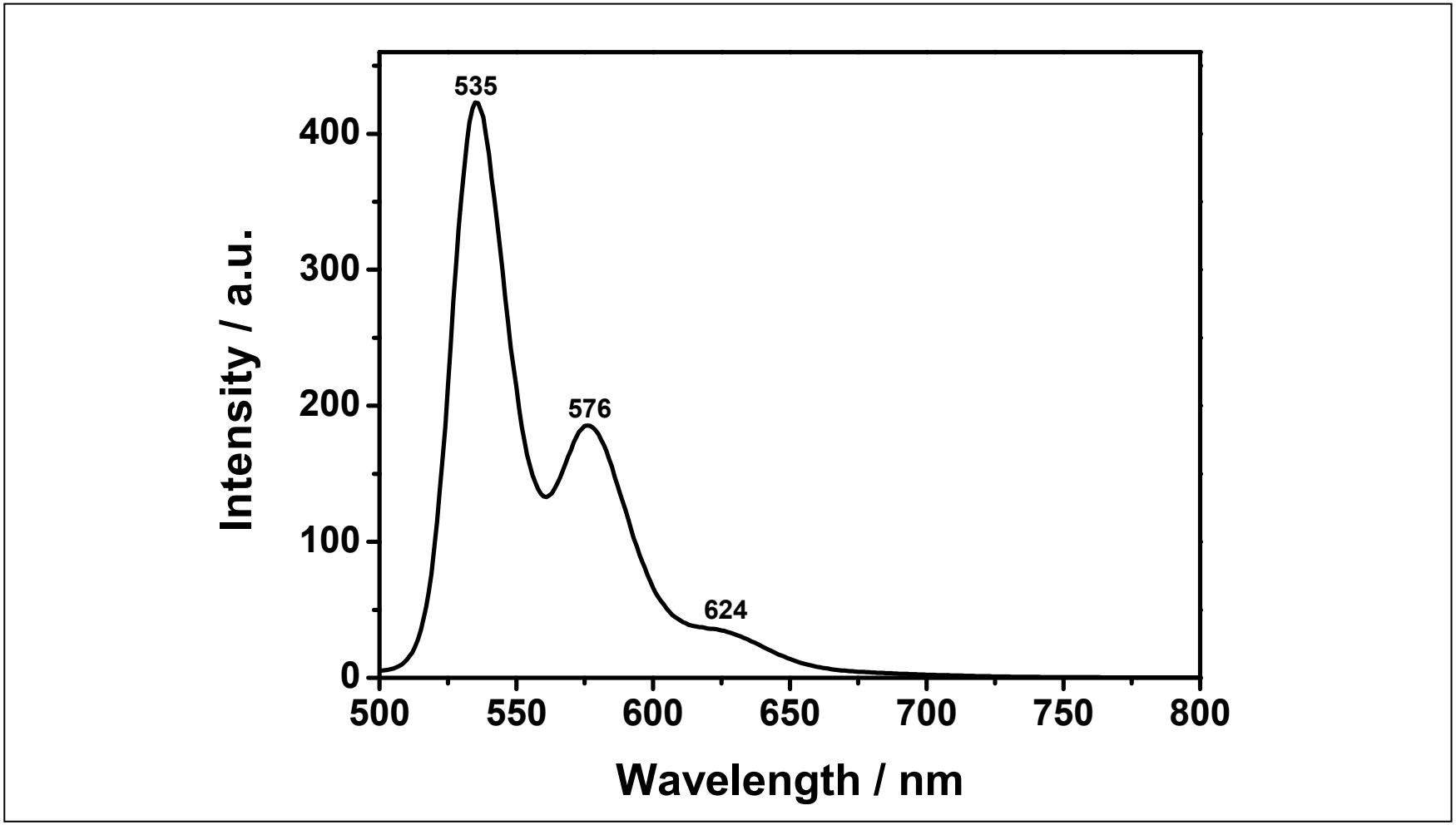

Figure 4.10: Emission Spectrum (λ_{exc} = 485 nm) of ADPDI in DMF

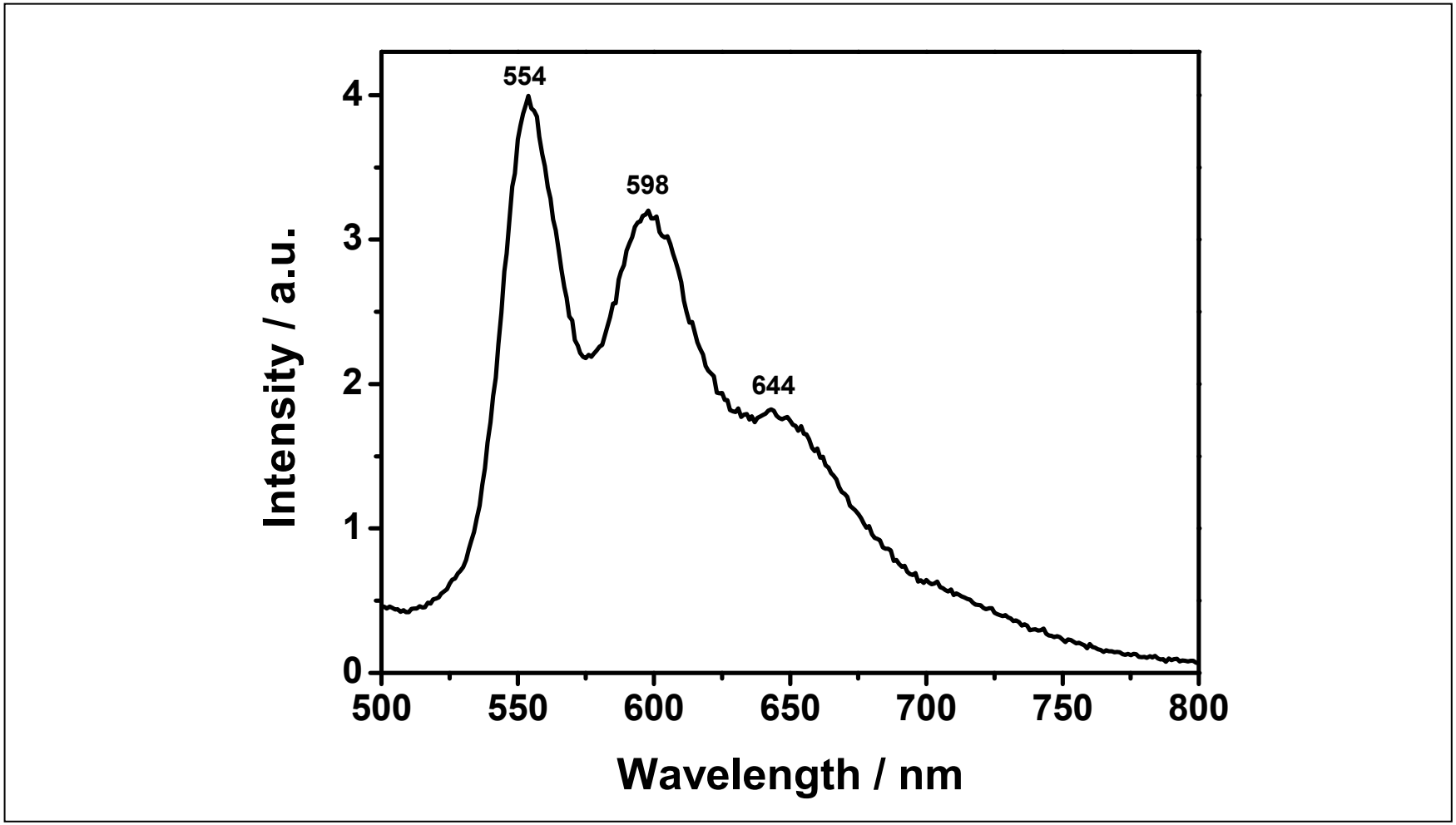

Figure 4.11: Emission Spectrum (λ_{exc} = 485 nm) of ADPDI in Isoquinoline

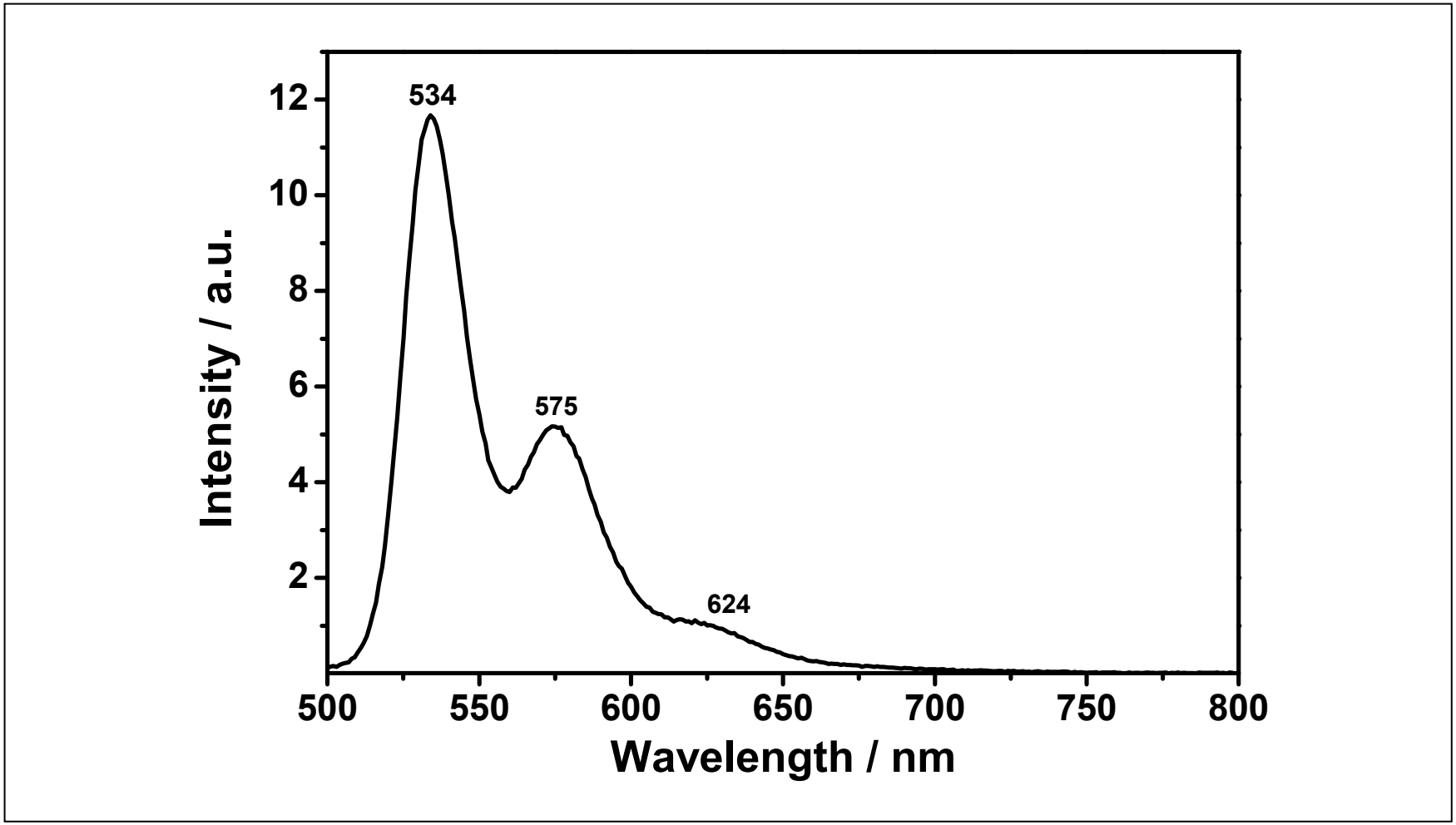

Figure 4.12: Emission Spectrum (λ_{exc} = 485 nm) of ADPMI in DMF

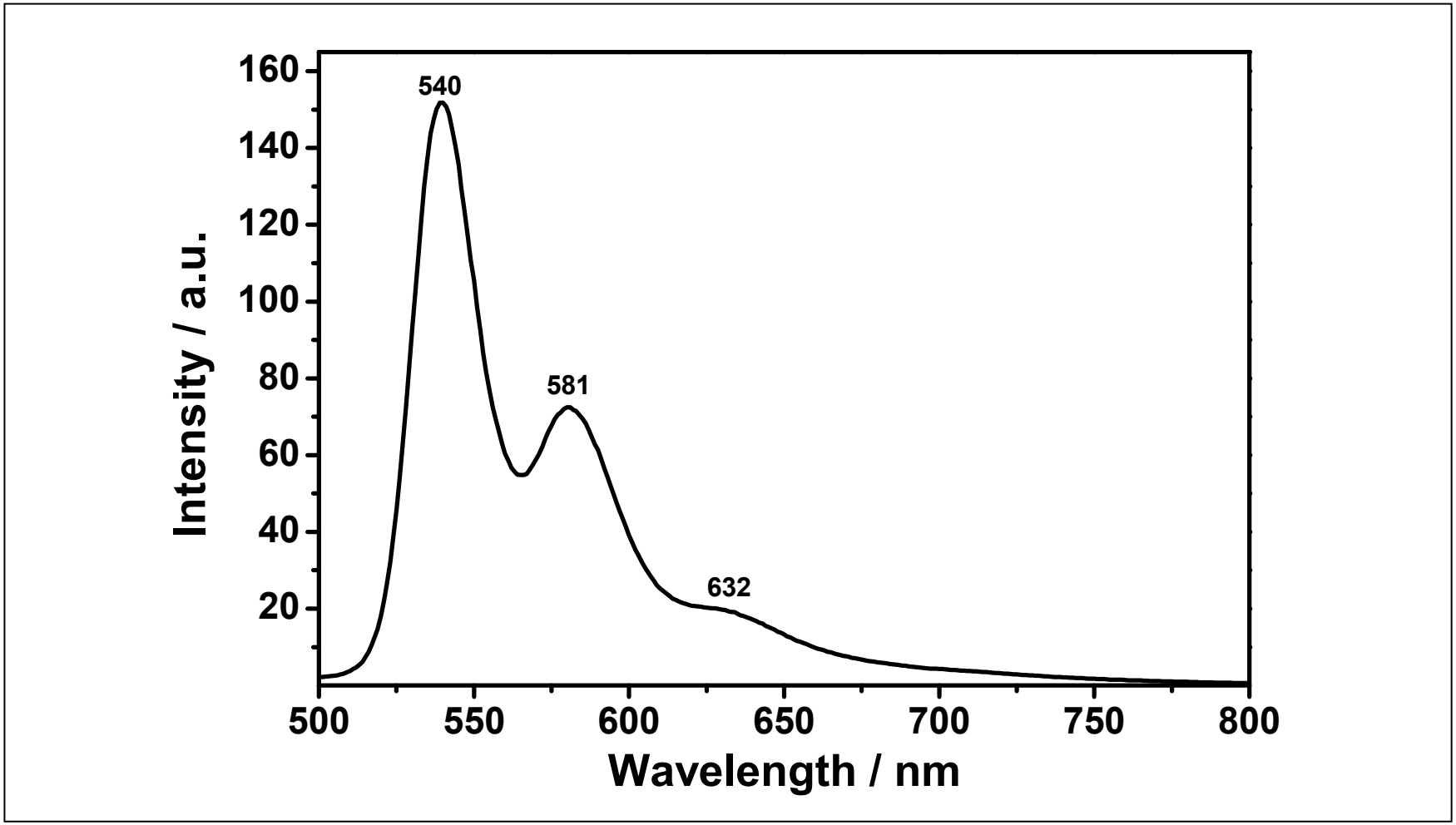

Figure 4.13: Emission Spectrum (λ_{exc} = 485 nm) of ADPMI in DMSO

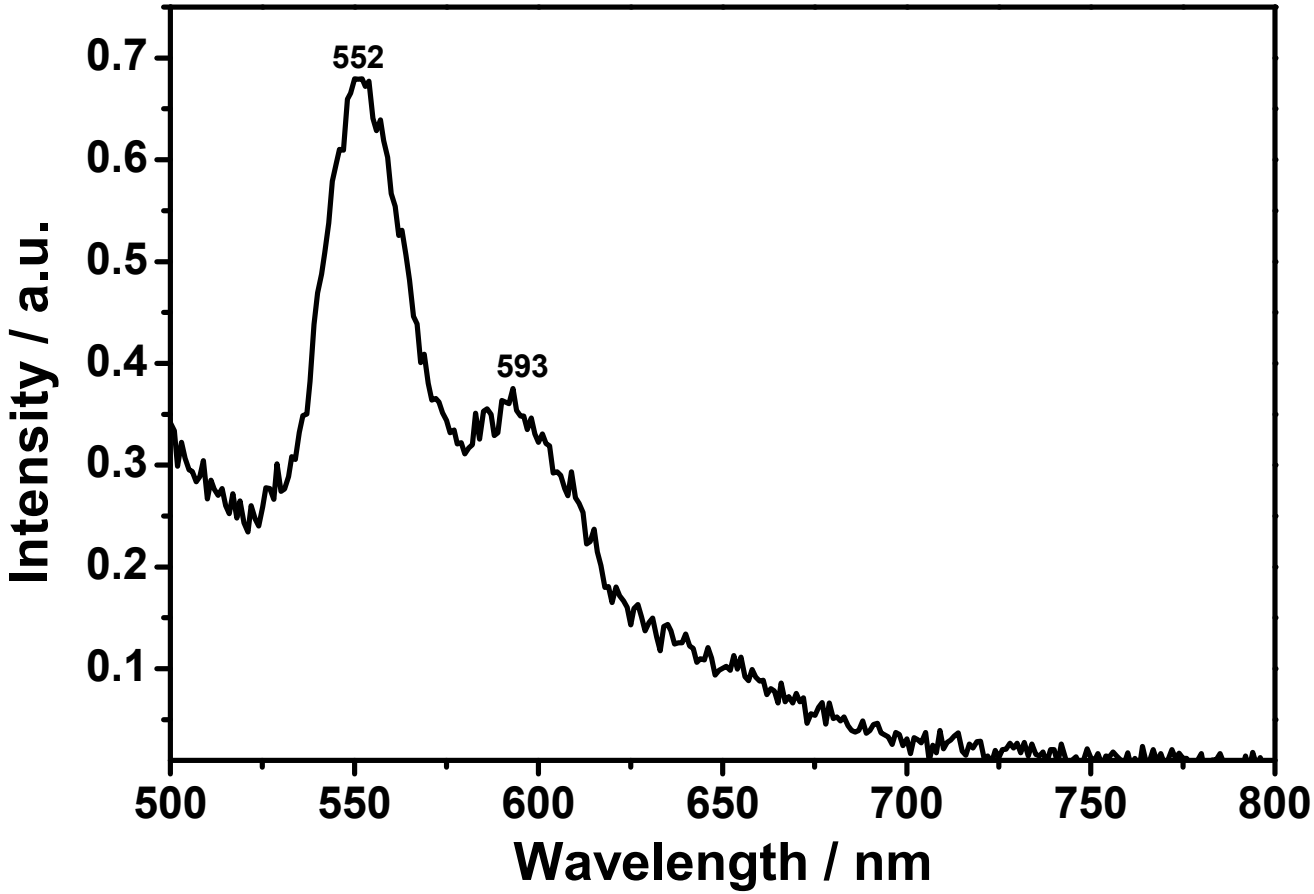

Figure 4.14: Emission Spectrum (λ_{exc} = 485 nm) of ADPMI in Isoquinoline

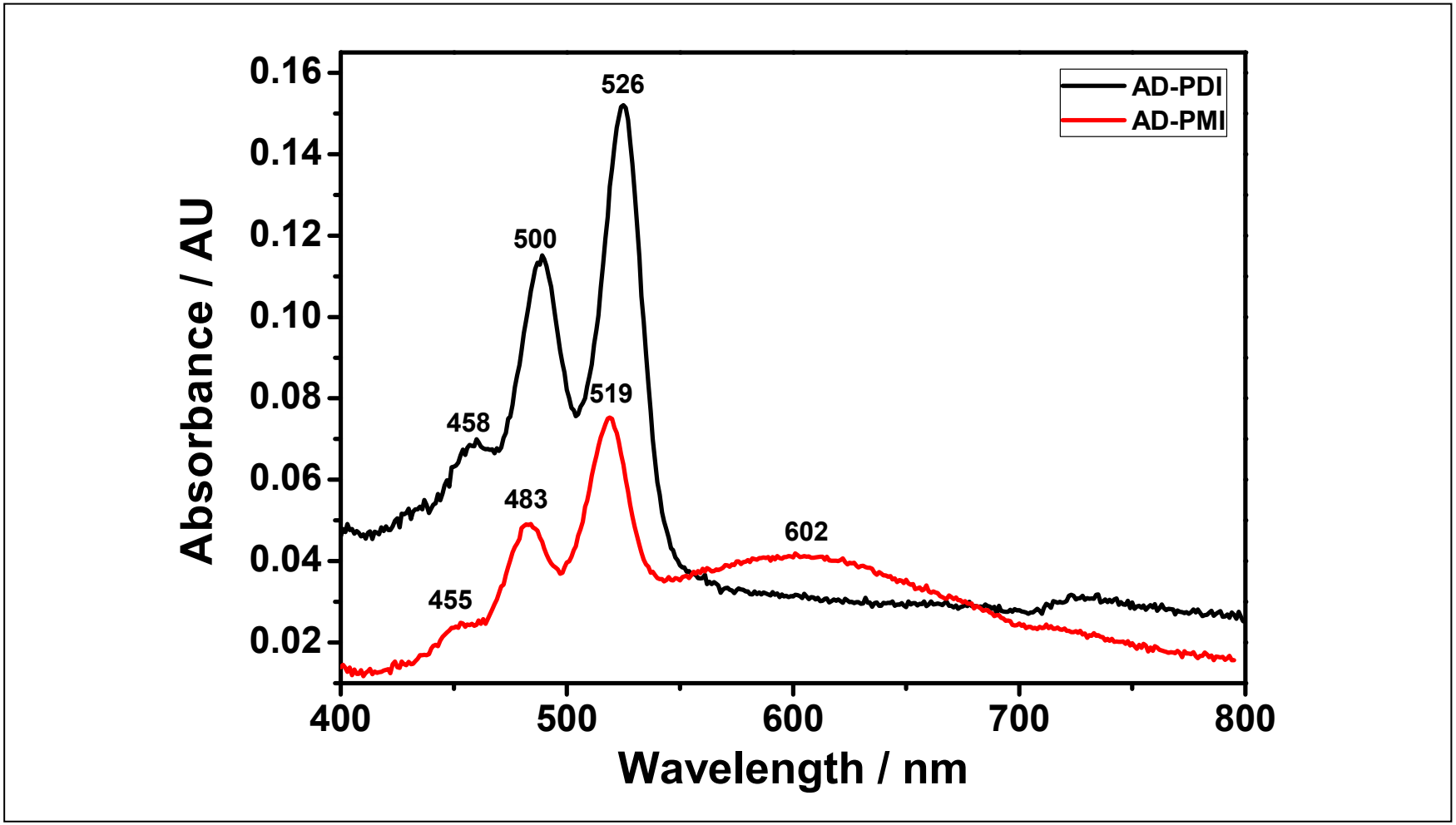

Figure 4.15: Absorption Spectra of ADPDI and ADPMI in DMF

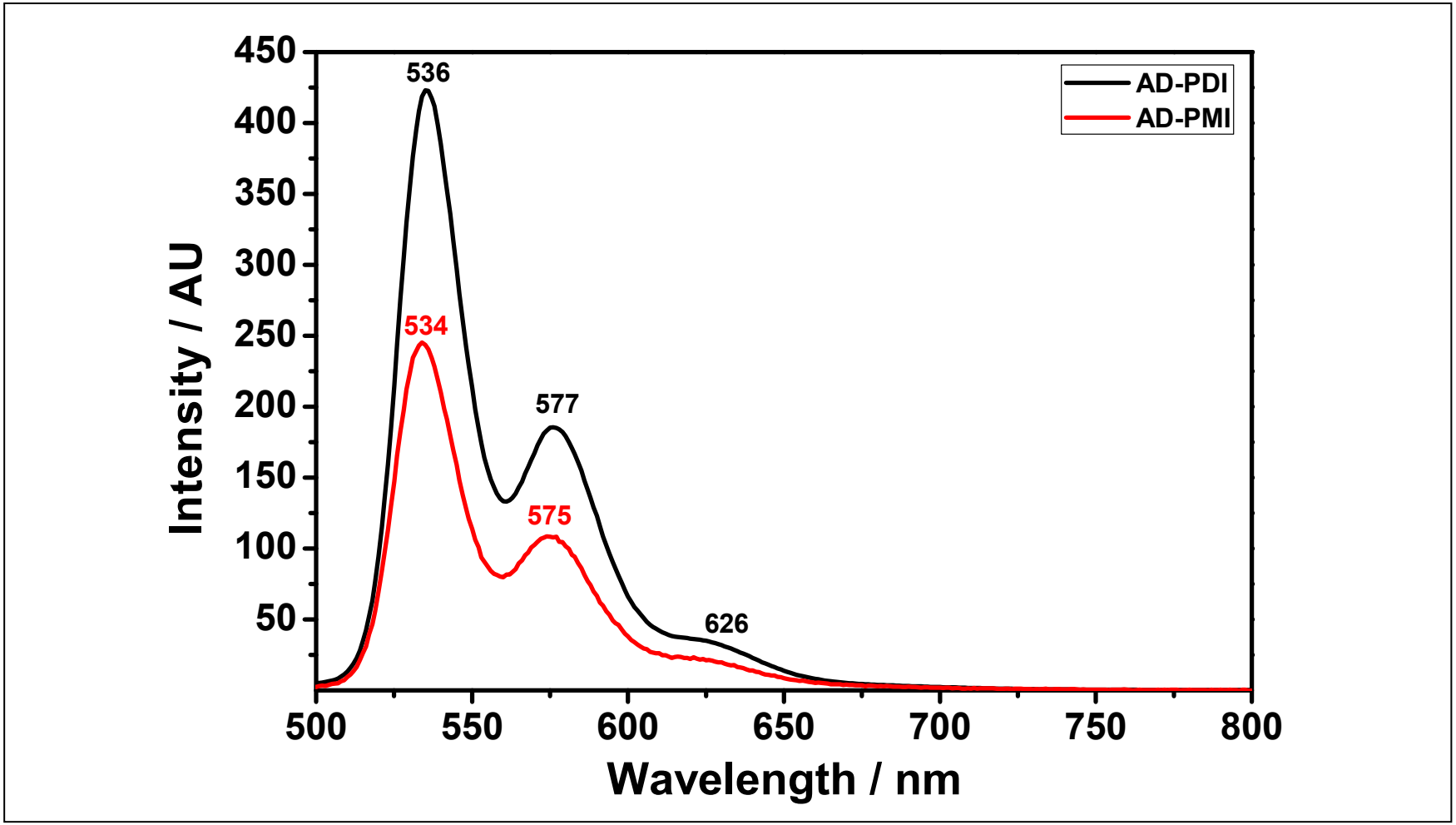

Figure 4.16: Emission Spectra (λ_{exc} = 485 nm) of ADPDI and ADPMI in DMF

Chapter 5

RESULTS AND DISCUSSION

5.1 Synthesis of Perylene Dyes

The synthesis of perylene dyes were successfully carried out using the previously reported methods [2–5, 20–23, 30]. Firstly, the perylene diimide dye was synthesized using the condensation reaction between the commercial compounds perylene-3,4,9,10-tetracarboxylic dianhydride and diaminododecane in presence of high boiling point solvents (*m*-cresol and isoquinoline). The reaction must be carried out at high temperatures and therefore these high boiling point solvents are employed in the reaction. Utmost care is taken for providing the argon atmosphere during the reaction and all the reagents were pre-dried before the synthesis with usual known drying methods. The reaction completion was regularly followed by TLC and FTIR spectroscopy. Common purification techniques were employed to purify the synthesized compound and the final product of perylene diimide dye was dried in the vacuum oven before exploring the detailed characterization of the dye. As mentioned earlier, the yield was high (84%).

Secondly, the perylene monoimide dye was synthesized by refluxing the prepared aminododecyl perylene diimide dye in presence of commercial reagents KOH, isopropanol. Generally, synthesis of perylene monoimide dyes involves complex procedure and the yields were generally low [21]. Icil's group has successfully synthesized various perylene monoimide dyes in high yields [31, 32]. The present

aminododecyl perylene monoimide was also synthesized in high yield (80%). The crucial step in the synthesis was redissolving the crude product in KOH solution followed by washing with dilute acidic solution. Finally, the synthesized compound was dried in vacuum oven for its characterization.

5.2 Characterization of Perylene Dyes

5.2.1 Solubility

The perylene dyes usually suffer from low solubilities due to their rigidity. The problem can usually overcome by attaching long alkyl chains or bulky groups at imide positions or substitution of various moieties in the bay region of perylene chromophore. The present aminododecyl perylene imide dyes have shown good solubility in dipolar aprotic solvents (except ADPDI in DMSO) and are insoluble in low polar and polar protic solvents (Table 5.1). This could be due to the primary amine groups present in the structure making the overall compound highly polar. However, ADPDI has shown enough solubility (spectroscopic) to measure fluorescence quantum yield.

Table 5.1: Solubility of Synthesized Aminododecyl Perylene Dyes

solubility/color data of perylene dyes		
solvent	**ADPDI**	**ADPMI**
Chloroform	partially soluble (low) / pink	insoluble
DMF	partially soluble / light purple	partially soluble / purple
DMSO	insoluble	partially soluble / purple
isoquinoline	completely soluble / dark brown	completely soluble / dark brown

The solubility in dipolar aprotic solvents is used to characterize the optical properties of the synthesized compounds.

5.2.2 Thin Layer Chromatography Characterization of ADPDI and ADPMI

The synthesized compounds were characterized by thin layer chromatography and the picture is shown below (Figure 5.1).

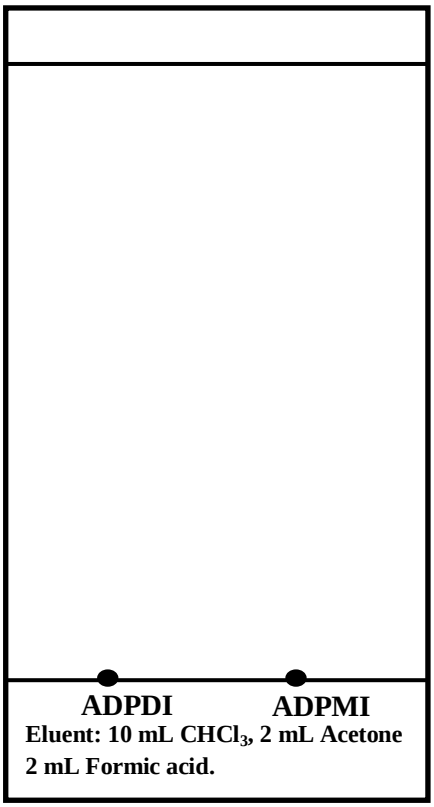

Figure 5.1: Thin Layer Chromatography of ADPDI and ADPMI

The two synthesized compounds were spotted on the silica coated thin layer chromatography plate. The eluent (10 mL $CHCl_3$ + 2 mL acetone + 2 mL formic acid) was run into the TLC plate. As shown in the diagram, the compounds did not move from the baseline. The R_f value was estimated as zero due to the stationary spots of two compounds. This is due to the high polar nature of the compounds which contain the long alkyl chains with primary amine groups (Figures 1.6 and Figures 1.7).

5.2.3 Characterization of FTIR Spectra

Figures 4.3 and 4.4 show the FTIR spectra of ADPDI and ADPMI, respectively. The FTIR spectrum of ADPDI (Figure 4.3) has shown characteristic functional group stretching and bending vibrations at: 3304 cm^{-1} (broad N–H stretching), 3059 cm^{-1} (aromatic C–H stretching), 2922, 2850 cm^{-1} (aliphatic C–H stretchings), 1696, 1655 cm^{-1} (imide C=O stretchings), 1596, 1579 cm^{-1} (aromatic C=C stretching), 1342 cm^{-1} (C–N stretching), and 809, 746 cm^{-1} (aromatic C–H bending), respectively.

The FTIR spectrum of ADPMI (Figure 4.4) has shown characteristic functional group stretching and bending vibrations at: 3404 cm^{-1} (broad N–H stretching), 2926, 2854 cm^{-1} (aliphatic C–H stretchings), 1777, 1730 cm^{-1} (anhydride C=O stretchings), 1696, 1652 cm^{-1} (imide C=O stretchings), 1595 cm^{-1} (aromatic C=C stretching), 1404 cm^{-1} (aliphatic C–H bending), 1092 cm^{-1} (C–O–C stetching), and 948, 809 cm^{-1} (aromatic C–H bending), respectively.

The most important characteristic differences between the two FTIR spectra of ADPDI and ADPMI have been noticed at: 1696, 1655 cm^{-1} (presence of imide C=O stretchings and absence of anhydride C=O stretchings) representing ADPDI (Figure 4.3); on the other hand 1777, 1730 cm^{-1} (anhydride C=O stretchings), 1696, 1652 cm^{-1} (imide C=O stretchings) representing ADPMI (Figure 4.4). In addition, strong C–O–C stetching has been noticed for ADPMI only. These characteristic differences prove both the structures of ADPDI and ADPMI.

5.3 Optical Properties

The optical characterization of ADPDI and ADPMI are explored through UV-vis absorption spectra and emission spectra. Various optical parameters are calculated from the data obtained through the UV-vis absorption and emission spectra and are presented in Tables 4.1 – 4.8. The measurements have been carried out in the solvents where the solubility is appreciable.

5.3.1 Characterization of Absorption Spectra

The absorption spectra of aminododecyl perylene diimide (ADPDI) in different solvents are shown in Figures 4.5, 4.6 and 4.15. Figure 4.5 shows the absorption spectrum of ADPDI in dipolar aprotic solvent, DMF. The absorption spectrum shows three characteristic peaks of perylene chromophore at 458, 500, and 526 nm, respectively. These three peaks are due to the $\pi \rightarrow \pi^*$ electronic transitions from ground state to the excited states representing the $0 \rightarrow 2$, $0 \rightarrow 1$, and $0 \rightarrow 0$ transitions, respectively.

Figure 4.6 shows the absorption spectrum of ADPDI in nonpolar solvent, isoquinoline. Interestingly, the absorption spectrum shows two characteristic $\pi \rightarrow \pi^*$ electronic transition peaks of perylene chromophore at 501 and 540 nm, respectively. Additionally, a broad shoulder at 590 nm is noticed which could be attributed to the probable aggregation and intermolecular hydrogen bonding of the solvent molecules with the ADPDI molecules. When compared to the absorption spectrum of ADPDI in DMF, a red shift of 14 nm is noticed for absorption in isoquinoline (for $0 \rightarrow 0$ transition, Figures 4.5 and 4.6).

The molar absorption coefficient values of ADPDI have been calculated and shown in Tables 4.2 and 4.4. The ε_{max} values (for 0→0 transition) are 22000 and 47000 $M^{-1} \cdot cm^{-1}$ in DMF and isoquinoline, respectively.

The absorption spectra of aminododecyl perylene monoimide (ADPMI) in different solvents are shown in Figures 4.7 – 4.9, and 4.15. Figure 4.7 shows the absorption spectrum of ADPMI in dipolar aprotic solvent, DMF. The absorption spectrum shows three characteristic peaks of perylene chromophore at 455, 483, and 519 nm, respectively. These three peaks are due to the π→π* electronic transitions from ground state to the excited states representing the 0→2, 0→1, and 0→0 transitions, respectively. In addition, a broad shoulder peak is noticed at 602 nm. When compared to the absorption spectrum of ADPDI in DMF, ADPMI has shown a blue shift of 7 nm for the 0→0 transition. Moreover, ADPDI has shown no additional shoulder band in its absorption spectrum of DMF (Figure 4.5 and 4.15). The strong additional shoulder absorption band for ADPMI in DMF is probably due to the aggregation of ADPMI molecules in solution. ADPMI is a polar molecule with anhydride and amine moieties and is explained from its thin layer chromatography characterization. In dipolar aprotic solvent DMF, ADPMI is probably more polarized causing aggregation. Interestingly, the absorption spectrum of ADPMI in DMSO has shown weak additional shoulder band in addition to the characteristic three perylene π→π* absorption peaks at 458, 487, and 522 nm, respectively (Figure 4.8). This shows that ADPMI was not polarized as much as in DMF. A representative comparison of absorption spectra of ADPDI and ADPMI in DMF has been explored in Figure 4.15.

Figure 4.9 shows the absorption spectrum of ADPMI in nonpolar solvent, isoquinoline. The absorption spectrum is similar to the absorption spectrum of ADPDI in isoquinoline as ADPMI also shows two characteristic $\pi \rightarrow \pi^*$ electronic transition peaks of perylene chromophore at 495 and 531 nm, respectively (Figures 4.6 and 4.9). However, the additional shoulder absorption band for ADPMI is broader when compared to the similar shoulder band of ADPDI in isoquinoline solution. This could be again attributed to the structural difference of ADPMI from ADPDI where the former contains additional anhydride moiety. This allows more probable intermolecular hydrogen bonding with the anhydride, amine moieties and solvent molecules. When compared to the absorption spectrum of ADPMI in DMF, a red shift of 12 nm is noticed for absorption in isoquinoline (for $0 \rightarrow 0$ transition).

The molar absorption coefficient values of ADPMI have been calculated and shown in Tables 4.2 and 4.4. The ε_{max} values (for $0 \rightarrow 0$ transition) are 19000, 47000 and 45000 $M^{-1} \cdot cm^{-1}$ in DMF, isoquinoline, and DMSO, respectively.

FWHM data, relative theoretical radiative lifetime values (τ_0), strength of absorption–oscillator strength (f), singlet energy data for both synthesized ADPDI and ADPMI compounds in various solvents were estimated and presented in Tables 4.3, 4.4, 4.7 and 4.8, respectively. ADPDI has shown higher theoretical radiative lifetimes when compared to ADPMI.

5.3.2 Characterization of Emission Spectra

The emission spectra of both ADPDI and ADPMI compounds have been explored through Figures 4.10 – 4.14, and 4.16. Both the compounds in various solvents have been studied at excitation wavelength of 485 nm (λ_{exc} = 485 nm).

Figure 4.10 shows emission spectrum of ADPDI in DMF. The emission spectrum shows three characteristic emission peaks representing the perylene chromophoric emission of 0→0, 0→1, and 0→2 transitions at 535, 576, and 624 nm, respectively. The emission spectrum is like the mirror image of its absorption spectrum (Figure 4.5 and 4.10).

Figure 4.11 shows the emission spectrum of ADPDI in isoquinoline. The spectrum is broader when compared to the emission spectrum of ADPDI in DMF. The behavior is relevant to the same additional broadness observed in their corresponding absorption spectra (Figures 4.5 and 4.6, where the absorption of ADPDI is broader in isoquinoline). The spectrum contains three characteristic emission peaks at 554, 598, and 644 nm, respectively. Interestingly, the emission spectrum is not a clear mirror image of its corresponding absorption spectrum (Figures 4.6 and 4.11). When compared to the emission spectrum of ADPDI in DMF, a red shift of 19 nm is noticed in isoquinoline solution (for 0→0 transition, Figures 4.10 and 4.11).

The emission spectrum of ADPMI in DMF shows three characteristic emission peaks at 534, 575, and 624 nm, respectively (Figure 4.12). Interestingly, the emission spectrum is not a clear mirror image of its corresponding absorption spectrum (Figures 4.7 and 4.12). Only, the perylene core peaks (the three characteristic absorption and emission peaks) have shown some mirror image and the additional

broad absorption shoulder band that noticed has no impact on its corresponding emission (Figures 4.7 and 4.12). Interestingly, the emission spectrum of ADPMI in DMF has shown no change when compared to the emission spectrum of its corresponding diimide entity (ADPDI) in the same DMF solvent regardless of the differences in their corresponding absorption spectra of both compounds (*see* Figures 4.15, 4.16, 4.5 and 4.7, Figures 4.10 and 4.12).

Figure 4.13 shows the emission spectrum of ADPMI in DMSO. The spectrum shows three characteristic emission peaks resembling the peaks from their emission spectra in DMF solution at 540, 581, and 632 nm, respectively. However, the emission spectrum in DMSO has shown a red shift of 6 nm for the 0→0 transition when compared to the emission in DMF solution.

Figure 4.14 shows the emission spectrum of ADPMI in isoquinoline. Interestingly, the emission is not a mirror image of its corresponding absorption spectrum (Figures 4.9 and 4.14). Moreover, the emission is broader and only emitted two characteristic perylene core emission peaks at 552 and 593 nm. When compared to the emission spectrum of ADPMI in DMF, a red shift of 18 nm is noticed in isoquinoline solution (for 0→0 transition, Figures 4.12 and 4.14). The emission spectral shape of ADPMI in isoquinoline is also different from its structural analogue of diimide dye (ADPDI) in the same solvent (isoquinoline) where the latter has shown characteristic three perylene core emission peaks. The representative comparison in emission of both ADPDI and ADPMI has been presented in Figure 4.16. As seen earlier, the differences in absorption spectra (*see* Figure 4.15) of ADPDI and ADPMI have no impact on their corresponding emission spectra (*see* Figure 4.16).

The fluorescence quantum yields of both synthesized ADPDI and ADPMI compounds were calculated as 0.83 and 0.39 in chloroform and DMF, respectively. The result is in support of the reported fluorescence quantum yields of perylene diimide and monoimide dyes [2–5, 20–23, 30]. The fluorescence rate constants (k_f), theoretical Fluorescence Lifetime (τ_f), and rate constant of radiationless deactivation (k_d) were estimated by using the data of fluorescence quantum yields and were tabulated in Tables 4.5 and 4.6.

Chapter 6

CONCLUSION

The designed perylene dyes involving perylene chromophore and long alkyl amino chains (termed as aminododecyl perylene diimide, ADPDI and aminododecyl perylene monoimide, ADPMI) have been successfully synthesized in high yields. Generally, the yields of perylene monoimides are low. But, a careful methodology led to a high yield in the present synthesis.

The synthesized compounds were characterized by thin layer chromatography (TLC) to learn their R_f values, FTIR to prove the structure by elucidating the major functional groups, UV-vis and emission spectral measurements to explore the optical properties and optical parameters.

The synthesized perylene diimide and monimide dyes have found stationary during the TLC test even in the polar eluent (used formic acid). The result shows the high polar nature of the synthesized compounds which is relevant to their structure as they have primary amine groups.

FTIR spectra of the synthesized ADPDI and ADPMI compounds proved the characteristic stretching and bending vibrational absorption peaks of major functional groups. Especially, they both have shown a clear difference in their spectra as ADPDI has shown only imide functional group vibrations, whereas, ADPMI has

shown both imide and anhydride functional group vibrations in support of their structures, respectively.

The synthesized compounds have shown appreciable solubility mostly in dipolar aprotic solvents such as DMF and DMSO. However, both the compounds have shown complete solubility in nonpolar isoquinoline.

The absorption spectra of ADPDI in the solvents DMF and isoquinoline have shown characteristic perylene chromophoric electronic absorption peaks where the absorption in latter solution has shown additional absorption shoulder band at higher wavelengths representing the aggregation or probability of intermolecular hydrogen bonding.

Interestingly, ADPMI has shown the additional shoulder absorption band in both DMF and isoquinoline solutions in addition to the characteristic perylene chromophoric absorption peaks.

The molar absorptivity (ε_{max}) of ADPDI is comparatively higher when compared to the molar absorptivity of its corresponding structural analogue of perylene dye (ADPMI).

Generally, the emission spectra of both ADPDI and ADPMI have shown three characteristic emission peaks irrespective of the presence of additional absorption shoulder bands in their corresponding absorption spectra. The fluorescence quantum yield of ADPDI is high (0.83) and for ADPMI is moderate (0.39).

The future work of the present research is to improve the structural properties of perylene dyes by bringing the positive charge at its imide moieties to bind effectively to DNA. The further step is to bind the developed perylene dyes to DNA to form G-quadruplexes which will be tested by electrophoresis methodology (Figure 6.1).

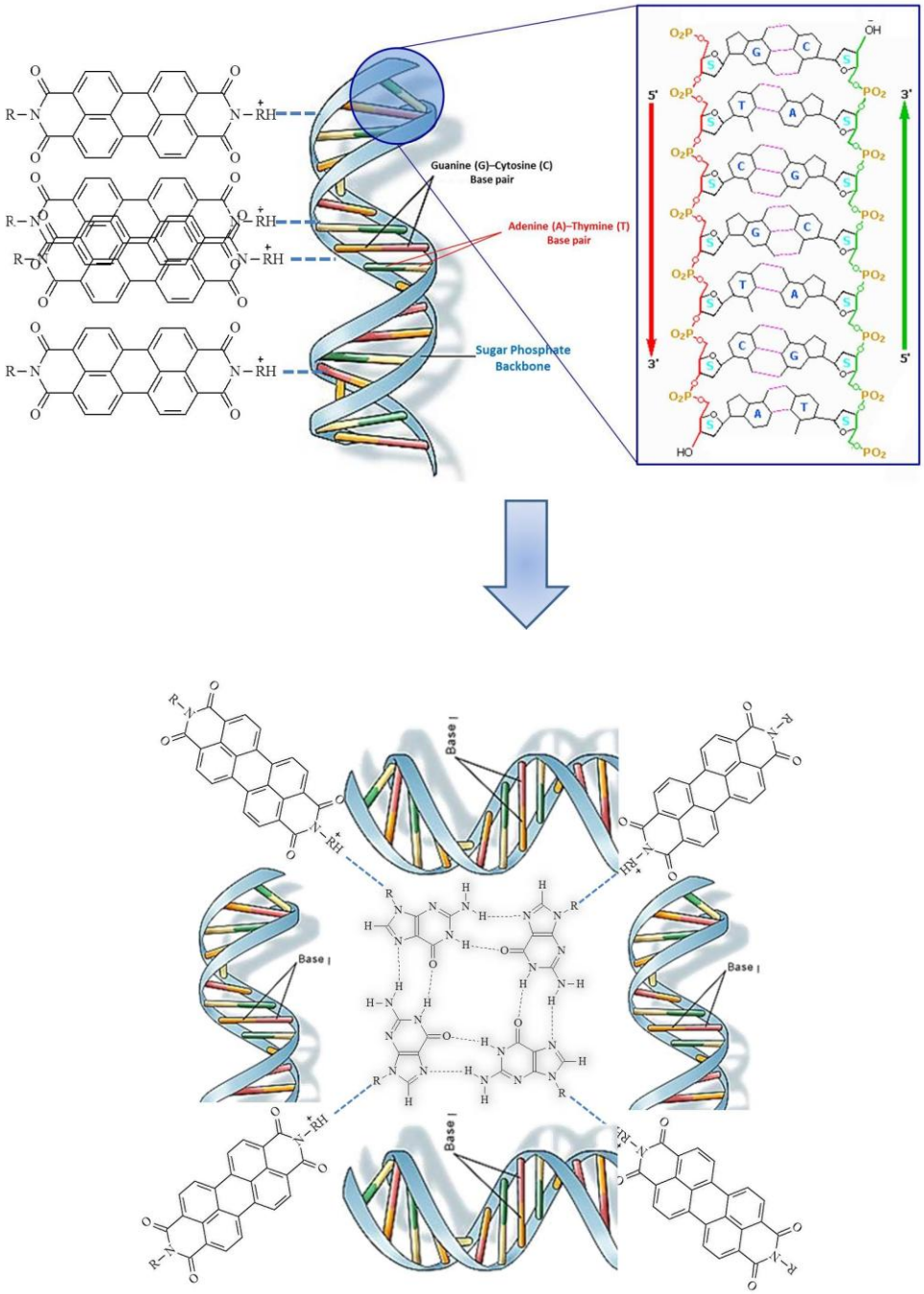

Figure 6.1: Representation of Perylene Dye – DNA Binding

REFERENCES

[1] Weil, T., Vosch, T., Hofkens, J., Peneva, K., & Müllen, K. (2010). The Rylene Colorant Family—Tailored Nanoemitters for Photonics Research and Applications. *Chem. Int.* 49, 9068–9093.

[2] Icil, H., & Icili, S. (1997). Synthesis and Properties of a New Photostable Polymer: Perylene-3,4,9,10-tetracarboxylic Acid–bis-(N,N'-dodecylpolyimide). *Journal of Polymer Science Part A: Polymer Chemistry.* 35, 2137–2142.

[3] Icil, H. (1998). Energy Transfer Studies with Perylene bis-Diimide Derivatives. *Spectroscopy Letters*. 31, 747–755.

[4] Bodapati, J. B., & Icil, H. (2008). Highly Soluble Perylene Diimide and Oligomeric Diimide Dyes Combining Perylene and Hexa(Ethylene Glycol) Units: Synthesis, Characterization, Optical and Electrochemical Properties. *Dyes and Pigments*. 79, 224–235.

[5] Ozdal, D., Asir, S., Bodapati, J. B., & Icil, H. (2013). Synthesis of a Novel Fluorescent Amphiphilic Chitosan Biopolymer: Photophysical and Electrochemical Behavior. *Photochem. Photobiol. Sci*. 12, 1927–1938.

[6] Hurley, L. H., Wheelhouse, R. T., Sun, D., Kerwin, S. M., Salazar, M., Fedoroff, O. Y., Han, F. X., Han, H., Izbicka, E., & Von Hoff, D. D. (2000). G-quadruplexes as Targets for Drug Design. *Pharmacology & Therapeutics*. 41, 141–158.

[7] Kerwin, S. M., Chen, G., Kern, J. T., & Thomas, P. W. (2002). Perylene Diimide G-quadruplex DNA Binding Selectivity is Mediated by Ligand Aggregation. *Bioorganic & Medicinal Chemistry Letters*. 12, 447–450.

[8] Samudrala, R., Zhang, X., Wadkins, R. M., & Mattern, D. L. (2007). Synthesis of a Non-Cationic, Water-Soluble Perylene Tetracarboxylic Diimide and its Interactions with G-quadruplex-Forming DNA. *Bioorganic & Medicinal Chemistry*. 15, 186–193.

[9] Xue, L., Ranjan, N., & Arya, D. P. (2011). Synthesis and Spectroscopic Studies of the Aminoglycoside (Neomycin)-Perylene Conjugate Binding to Human Telomeric DNA. *Biochemistry*. 50, 2838–2849.

[10] Han, H., & Hurley, L. H. (2000). G-quadruplex DNA: A Potential Target for Anti-Cancer Drug Design. *Trends in Pharmacological Science*. 21, 136–142.

[11] Huppert, J. L. (2008). Hunting G-quadruplexes. *Biochimie*. 90, 1140–1148.

[12] Haider, S. M., Parkinson, G. N., & Neidle, S. (2003). Structure of a G-quadruplex–Ligand Complex. *J. Mol. Biol.* 326, 117–125.

[13] Rossetti, L., Franceschin, M., & Bianco, A. (2002). Perylene Diimides with Different Side Chains are Selective in Inducing Different G-quadruplex DNA Structures and in Inhibiting Telomerase. *Bioorganic & Medicinal Chemistry Letters*. 12, 2527–2533.

[14] Rossetti, L., Franceschin, M., Schirripa, S., Bianco, A., Ortaggi, G., & Savino, M. (2005). Selective Interactions of Perylene Derivatives having Different Side Chains with Inter-and Intramolecular G-quadruplex DNA Structures. A Correlation with Telomerase Inhibition. *Bioorganic & Medicinal Chemistry Letters*. 15, 413–420.

[15] Hardin, C. C., Henderson, E., Watson, T., & Prosser, J. K. (1991). Monovalent Cation Induced Structural Transitions in Telomeric DNAs: G-DNA Folding Intermediates. *Biochemistry*. 30, 4460–4472.

[16] Conoci, S., Mascali, A., & Pappalardo, F. (2014). Synthesis DNA Binding Properties and Electrochemistry Towards an Electrode-Bound DNA of a Novel Anthracene–Viologen Conjugate. *RSC Adv.* 4, 2845–2850.

[17] Bowater, R. P., Davies, R. J., Palecek, E., & Fojta, M. (2009). Sensitive Electrochemical Assays of DNA Structure Electrochemical Analysis of DNA. *Chemistry Today*. 27, 50–54.

[18] Lee, J. K., Jung, Y. H., Tok, J. B., & Bao, Z. (2011). Syntheses of Organic Molecule-DNA Hybrid Structures. *ACS Nano*. 5, 2067–2074.

[19] Doluca, O., Withers, J. M., & Filichev, V. V. (2013). Molecular Engineering of Guanine-Rich Sequences: Z-DNA, DNA Triplexes, and G-quadruplexes. *Chem. Rev*. 113, 3044–3083.

[20] Uzun, D., Ozser, M. E., Yuney, K., Icil, H., & Demuth, M. (2003). Synthesis and Photophysical Properties of *N,N'*-bis(4-cyanophenyl)-3,4,9,10-Perylenebis(dicarboximide) and *N,N'*-bis(4-cyanophenyl)-1,4,5,8-Naphthalenediimide. *Journal of Photochemistry and Photobiology A: Chemistry*. 156, 45–54.

[21] Amiralaei, S., Uzun, D., & Icil, H. (2008). Chiral Substituent Containing Perylene Monoanhydride Monoimide and Its Highly Soluble Symmetrical Diimide: Synthesis, Photophysics and Electrochemistry from Dilute Solution to Solid State. *Photochemical & Photobiological Sciences*. 7, 936–947.

[22] Asir, S., Demir, A. S., & Icil, H. (2010). The Synthesis of Novel, Unsymmetrically Substituted, Chiral Naphthalene and Perylene Diimides: Photophysical, Electrochemical, Chiroptical and Intramolecular Charge Transfer Properties. *Dyes and Pigments*. 84, 1–13.

[23] Refiker, H., & Icil, H. (2011). Amphiphilic and Chiral Unsymmetrical Perylene Dye for Solid-State Dye-Sensitized Solar Cells. *Turk J. Chem*. 35, 847–859.

[24] Kern, J. T., & Kerwin, S. M. (2002). The Aggregation and G-quadruplex DNA Selectivity of Charged 3,4,9,10-Perylenetetracarboxylic Acid Diimides. *Bioorganic & Medicinal Chemistry Letters*. 12, 3395–3398.

[25] Mazzitelli, C. L., Brodbelt, J. S., Kern, J. T., Rodriguez, M., & Kerwin, S. M. (2006). Evaluation of Binding of Perylene Diimide and Benzannulated Perylene

Diimide Ligands to DNA by Electrospray Ionization Mass Spectrometry. *Journal of the American Society for Mass Spectrometry*. 17, 593–604.

[26] Tuntiwechapikul, W., Taka, T., Béthencourt, M., Makonkawkeyoon, L., & Randall Lee, T. (2006). The Influence of pH on the G-quadruplex Binding Selectivity of Perylene Derivatives. *Bioorganic & Medicinal Chemistry Letters*. 16, 4120–4126.

[27] Franceschin, M., Pascucci, E., Alvino, A., D'Ambrosio, D., Bianco, R., Ortaggi, G., & Savino, M. (2007). New Highly Hydrosoluble and Not Self-Aggregated Perylene Derivatives with Three and Four Polar Side-Chains as G-quadruplex Telomere Targeting Agents and Telomerase Inhibitors. *Bioorganic & Medicinal Chemistry Letters*. 17, 2515–2522.

[28] Franceschin, M., Lombardo, C. M., Pascucci, E., D'Ambrosio, D., Micheli, E., Bianco, A., Ortaggi, G., & Savino, M. (2008). The Number and Distances of Positive Charges of Polyamine Side Chains in a Series of Perylene Diimides Significantly Influence Their Ability to Induce G-quadruplex Structures and Inhibit Human Telomerase. *Bioorganic & Medicinal Chemistry*. 16, 2292–2304.

[29] Micheli, E., Lombardo, C. M., D'Ambrosio, D., Franceschin, M., Neidle, S., & Savino, M. (2009). Selective G-quadruplex Ligands: The Significant Role of Side Chain Charge Density in a Series of Perylene Derivatives. *Bioorganic & Medicinal Chemistry Letters*. 19, 3903–3908.

[30] Icil, H., & Arslan, E. (2001). Synthesis and Spectroscopic Properties of Highly Pure Perylene Fluorescent Dyes. *Spectroscopy Letters*. 3, 355–363.

[31] Pasaogullari, N., Icil, H., & Demuth, M. (2006). Symmetrical and Unsymmetrical Perylene Diimides: Their Synthesis, Photophysical and Electrochemical Properties. *Dyes and Pigments*. 69, 118–127.

[32] Ahmed, H. (2013). Eastern Mediterranean University, MS Thesis.